U.S. DEPARTMENT OF COMMERCE / Environmental Science Services Administration
Coast & Geodetic Survey

SEISMIC ANALYSIS OF A NUCLEAR EXPLOSION

GASBUGGY

December 10, 1967

B. G. Reagor
D. W. Gordon
J. N. Jordan

Prepared for
Advanced Research Projects Agency
Nuclear Test Detection Office
ARPA Order No. 1095

October 1968

82

SEISMIC ANALYSIS OF A NUCLEAR EXPLOSION

G A S B U G G Y

10 December 1967

ARPA Order No.:	1095 Amendment No. 1
ARPA Program Code No.:	8F10
ARPA Program Element Code:	6.25. 06.01. D
Industrial Priority Rating:	DO
Name:	ESSA/Coast and Geodetic Survey Seismology Division
Date of Contract:	12 March 1968
Principal Investigator:	James N. Jordan Special Seismological Analysis Branch (301) 49-68356 IDS 14-68356
Project Geophysicists:	B. G. Reagor D. W. Gordon

AVAILABILITY

Qualified Users May Request Copies of This Document From:

Defense Documentation Center
Cameron Station
Alexandria, Virginia 22314

or

Clearinghouse
Sills Building
5285 Port Royal Road
Springfield, Virginia 22151

TABLE OF CONTENTS

TABLE

TABLES (con.)

FIGURE

FIGURES (con.) Page

APPENDIX

ABSTRACT

A comparative study between GASBUGGY and GNOME data shows considerable differences in observed travel times, amplitudes, and in the excitation of surface waves. The Pn and P arrivals from GASBUGGY follow the Jeffreys-Bullen curve closely, whereas the arrival times for GNOME were early to the east and late to the west. Relatively higher amplitudes of phases associated with Pg and Lg were recorded to the east of GASBUGGY, whereas Pn and P and surface waves (LR) recorded higher amplitudes to the west of GASBUGGY. Rayleigh waves were strongly recorded at large distances from GASBUGGY with an average magnitude of 4.09, as compared with a M_B and M_E of 5.21 and 4.73, respectively. Since P and PKP data were not recorded beyond 86 degrees, the body wave magnitude computed according to Evernden (M_E) appeared to be a more reasonable value. A refinement of the GASBUGGY location was attempted by adjusting the arrival times relative to the residuals observed from GNOME. The maximum epicentral error increased approximately 7 kilometers to the north and 22 kilometers to the west.

INTRODUCTION

Project GASBUGGY, the first cooperative Government-industry Plowshare project, was detonated 10 December 1967 at 19h 30m 00.1s U.T. at a depth of 4240 feet in a shale environment. The 26-kiloton nuclear explosion was located in the San Juan Basin near Farmington, New Mexico. The geographic coordinates were 36°40'40.4" N, 107°12'30.3" W. The primary purpose of the experiment was to test a proposed method of increasing the production of oil and gas.

In this report the results of GASBUGGY will be compared with data from GNOME, an underground explosion detonated in a salt mine near Carlsbad, New Mexico. Apparently due to its location on the boundary between the Great Plains and the Rocky Mountains, GNOME exhibited considerable differences between amplitude attenuation and seismic velocities associated with wave propagation to the east and to the west of the test site. In contrast, the GASBUGGY site, which was located approximately 4°N and 3°W of GNOME, lies well within the Rocky Mountain region. One of the principal objectives of this report will be to determine the effect of shifting the test site several hundred kilometers to the west in a region where rapid changes in crustal and upper mantle structure are suspected.

GENERAL GEOLOGY

The GASBUGGY test site was located in the east-central portion of the San Juan Basin. The basin, approximately 90 miles in diameter, an area of about 10,600 miles, has an estimated 6000 feet of structural relief. Geologic formations exceeding 15,000 feet in total thickness range from pre-Cambrian age to Eocene in the interior part of the basin. The basin is rimmed by monoclines on the north, east, and west. The rocks in the southern part of the basin indicate periods of diastrophism, including folding, faulting, and igneous activity.

DISCUSSION OF DATA

GASBUGGY travel times were available from 157 stations, and ground amplitudes were determined at 129 stations where instrumental responses are well known. The closest station was at a distance of 44 kilometers from the test site, and the most distant was 9467 kilometers at Matsushiro, Japan. Seismic data were recorded from 19 stations outside of the North American Continent--two each in Greenland, South America, Finland, Sweden, and Japan, and nine in Europe.

Much of the travel-time information came from the World-Wide standard seismograph stations and other similar permanent observatories operated by universities and the Coast and Geodetic Survey. At distances less than 500 kilometers, 14 temporary stations operated by the Coast and Geodetic Survey and the

Geological Survey provided important supplemental travel times. In this report, only ten stations contributed useable data. The temporary station operational data are summarized in Appendix I. The temporary stations were equipped with high- and low-gain, three-component ASC1* and ASC2* Seismic Data Systems. To aid in the comparison with the GNOME event, LRSM data are included in the various diagrams. The LRSM stations were equipped with three-component short- and long-period instruments. The horizontals were oriented radially and transverse to the great circle path from the GASBUGGY epicenter.

The basic data used in this report are summarized in Figures 1, 2, and in Table 1. Figure 1 shows the geographic location of North American stations and type of signal reception at the stations known to have recorded GASBUGGY. Figure 2 shows reception characteristics at other teleseismic stations. In Table 1, the basic data includes distance (degrees and kilometers), instrumental component, phase identification, arrival time (uncorrected for ellipticity and station elevation), period and representative amplitude of selected phases, and both Gutenberg-Richter body-wave magnitude and the magnitude defined by Evernden (1967) which relates regional apparent velocities with representative amplitude attenuation. The Jeffreys-Bullen residual (observed-computed) takes into account the ellipticity and elevation correction for the longitudinal phases. Figure 3 illustrates signal detection

*Portable magnetic tape systems designed and built by Albuquerque Seismological Center (C&GS)

as a function of instrumental magnification and distance. As seen previously, there was considerable overlap of reception and nonreception at similar distances, which indicates signal detection is not a simple function of range and instrumental magnification. Other factors, such as the signal-to-noise ratio and the pattern of regional amplitude anomalies, appear to play an important role.

In the accompanying graphs of the data, which correspond to the phases Pn and P, Pg, Lg, and LR, the stations to the east of the test site are separated from those to the west by different symbols. This separation roughly approximates the division of the Continental United States into two major seismic provinces as delineated by the Rocky Mountain Front. The R^{-3} reference attenuation line was visually fitted to the data.

AMPLITUDES - TRAVEL TIMES

Pn and P

Amplitudes of the largest motion in the first three cycles are illustrated in Figure 4. The attenuation rate of the waves appeared to fit the R^{-3} reference line out to 700-800 kilometers as has been observed in the case of the NTS events. Beyond this point there was no apparent correlation, of course, as phases

representing deeper penetration became first arrivals.

As will be seen in this report, estimates of amplitude attenuation rates at regional distances consist of (1) matching the identified phase with an appropriate apparent velocity; (2) determining the amplitude decay associated with the corresponding refractor.

Several differences were noted when GNOME and GASBUGGY data were compared. The higher amplitudes of the eastern stations at similar distances to those to the west as observed for GNOME were not reflected by the GASBUGGY data. Generally, the stations to the west tended to have equal or higher amplitudes.

As shown in Figure 5, the arrival times of GASBUGGY followed the Jeffreys-Bullen curve closely. GNOME, in the distance range of 1000 kilometers, reported eastern stations about 5 sec early, as compared with 3 sec for GASBUGGY. Arrival times to the west of GASBUGGY showed a more striking disagreement in the distance range of 1000 to 1500 kilometers. GNOME reported a maximum residual of +4 sec whereas GASBUGGY reported a maximum of +2.5 sec. Also, a significant number of stations to the west of GASBUGGY reported early arrival times, whereas stations west of GNOME generally reported late arrivals.

At distances beyond 20 degrees, the average recorded arrival times were about 1.0 sec earlier than the travel times predicted

by the Jeffreys-Bullen table. Early arrival times were also observed from the GNOME explosion, as well as from earlier explosions in the Pacific area (Gutenberg and Richter, 1964; Burke-Gaffney and Bullen, 1957; Carder and Bailey, 1958; Carder, Gordon, and Jordan, 1966).

Travel-time data were available in the distance range from 44 to 9500 kilometers. All stations closer than 400 kilometers were located along a rough profile south of the test site. A straight-line approximation of the first leg (t_1) of the travel-time curve, corresponding to the arrival at station IRl at a range of 44 kilometers, yields an apparent velocity of 5.34 km/sec. The second branch of the travel-time curve, with an apparent velocity of 6.29 km/sec and a time axis intercept of 1.4 sec, corresponds to the observed first arrivals covering the 50 to circa 180 kilometers. Several investigations, including Carder, et. al., (1966) and Evernden (1967), have indicated that sub-Moho refractors, representing apparent velocities of 7.9, 8.5, and 10.5 km/sec, exist beneath the western United States. Reference lines representing these apparent velocities were visually fitted to the station data shown in Figure 5. As can be seen in Figure 5, there was considerable latitude, especially at the crossover points, in placing the reference lines through the data points. Possibly, the various apparent velocities associated with the stations recording first arrivals were

dependent upon the signal-to-noise amplitude ratio. In addition to the graphic representation in Figure 5 all travel times are presented in Table 2.

TABLE 2 -- Summary of Travel Times

Travel Time	Intercept	Surface Crossover (Distance km)
$t_1 = \Delta/5.34$		
$t_2 = \Delta/6.29$	+ 1.4	50
$t_3 = \Delta/7.9$	+ 7.0	155
$t_4 = \Delta/8.5$	+ 15.8	910

Regionalization was apparent when the station travel-time residuals were plotted and contoured on a map (Figure 6). The region of greatest negative residuals was located in the Mississippi River Valley, and the area of greatest positive residuals was located in the California area. This latter feature, although not as well defined as with GNOME, could represent the effect of the Sierra Nevada "root" projected on the surface to the west. The map generally agreed with the GNOME map, with the exception that GASBUGGY indicated negative residuals located in the Utah-Nevada area.

Figure 7 illustrates the patterns of maximum amplitudes of Pn and P waves across the United States. The contour interval

was based on the geometric progression 1, 2, 4, 8, 16, 32, etc., to permit contouring over the large range of observed amplitudes. Although the distance range was different for the two events, several geographic regions showed similar amplitude anomalies for GNOME and GASBUGGY. For example, the low-amplitude anomaly in Arkansas, at a distance of 1000 kilometers from GNOME, was repeated for GASBUGGY even though the distance was 1200 to 1400 kilometers. The high anomaly which occurred in Texas, 600 kilometers from GNOME, was not as well delineated by GASBUGGY. However, there was less control for GASBUGGY. The low-amplitude area which occurred in northern Colorado from GNOME had shifted northward from GASBUGGY but had still maintained the 1000-kilometer spacing. Also, as found in GNOME, GASBUGGY indicated low-amplitude anomalies in the California area and around the Nevada Test Site. Two high-amplitude anomalies were shown, due to greater station control by the recorded GASBUGGY data: One was 2800 kilometers to the northeast and the other 1700 kilometers to the northwest.

In Figure 7, the apparent velocities of the station first arrivals are indicated above the station code. At 1000 kilometers to the east of the GASBUGGY test site, the $P_{7.9}$ velocity arrival was replaced by the arrival of the $P_{8.5}$ refractor, and beyond 2000 kilometers, only the arrival with an apparent velocity of $P_{10.5}$ was recorded. To the west, the distinction

between the $P_{7.9}$ and $P_{8.5}$ apparent velocity arrivals were not as abrupt as it was to the east. In the distance range of 500 to 1000 kilometers, the identification of the $P_{7.9}$ velocity refractor was probably dependent upon a favorable signal-to-noise amplitude ratio at the individual stations. The appearance of the $P_{7.9}$ arrival, as suggested by Evernden (1967), could be distinctive in differentiating between the Eastern and Western United States. With the exception of WMO and GV-, the Rocky Mountain Front was roughly parallel to the alinement of stations which recorded the $P_{7.9}$ velocity arrival. As contrasted to the east where the $P_{10.5}$ velocity arrivals were observed only beyond 2000 kilometers, the $P_{10.5}$ arrival first appeared at a range of 1800 kilometers to the northwest.

The preliminary conclusion based on the station apparent velocity arrivals shows that the complexity of the upper mantle structure results in significant changes in the P-phase arrivals that cannot be accounted for by distance alone. As illustrated in Figure 7, the mantle structure is more complex toward the west as compared with the Eastern United States.

It was of interest to note that at <u>RCD</u> and WN-, the same distance, velocity refractor, and quadrant had striking differences in amplitudes. The low amplitude recorded at <u>RCD</u> could possibly be the result of a shadow effect associated with the Black Hills physiographic province.

Pg

As illustrated in Figure 8, Pg was evident out to a distance of 1630 kilometers to the east and 1400 kilometers to the west. The Pg amplitudes were generally higher toward the east than to the west, and the wave attenuation could be represented by the R^{-3} reference line out to 1000 kilometers, followed by a more rapid decay.

Lg

As shown by Figure 9, the wave attenuation appeared to follow the R^{-3} reference line. The Lg waves were recorded 3975 kilometers to the east and only 2911 kilometers to the west. Unlike GNOME, the stations to the east had higher amplitudes than those to the west. As with GNOME, the attenuation rate was less rapid toward the east than to the west.

It was of interest to note that Lg waves traversed the Hudson Bay and other shallow waters south of RES. This was indicated by the recorded Lg waves at both RES and FBC. This observation corresponded to the findings of Herrin (1960). Although a strong P signal was observed at MBC, Lg waves were not recorded. This verified the presence of an oceanic segment between the mainland and MBC.

LQ

Unlike GNOME, Love waves were recorded on WWNSS and LRSM

long-period instruments at maximum ranges of 2665 kilometers to the east and 1363 kilometers to the west. The period of Love waves ranged from 8 to 30 sec, with the dominant period about 15 sec. The horizontal component which recorded the wave form best is indicated by a special symbol in Figure 10. The wave attenuation rate appeared to be more rapid to the east than to the west.

LR

As observed from Figure 11, Rayleigh waves generated by GASBUGGY were recorded beyond 4000 kilometers to the east and 2000 kilometers to the west, whereas GNOME reported Rayleigh waves out to only 500 kilometers. The wave form designated LR had a duration of several cycles with a period of approximately 12 sec. At similar distances, in the distance range of 900 to 2000 kilometers, the stations to the west had higher amplitudes than the stations to the east.

BODY WAVE MAGNITUDES

Body wave magnitudes, corresponding to the P wave recorded by short-period vertical instruments, were computed according to the method given by Gutenberg and Richter (1956) and are shown in Figure 12. Note the scattering of data when the amplitude-distance relationships were applied to the calculation of body wave magnitudes. The average magnitude representing

stations at ranges less than 16 degrees is 5.20 and greater than 16 degrees the magnitude is 5.03. The value of 5.21 represents the overall average magnitudes.

A second plot of body wave magnitudes (Figure 13) has been prepared to show the effects of regional corrections suggested by Evernden (1967). In this plot, magnitudes in the range of 200 to 3000 kilometers were recomputed using "Q" factors which were generated by the formula $M_B = Q + q + S$, with reference to an event of magnitude 5, are listed in Appendix 2.

An average of all data, covering the entire distance range, gives a magnitude of 4.73. Stations beyond 16 degrees indicate a value of 4.99, whereas 4.52 represents the data obtained at less than 16 degrees. The application of the new set of "Q" factors did not completely remove the scatter in the magnitude data. In some instances, especially in the range of 1700 to 3000 kilometers, the adjusted reductions changed the magnitude residuals, either raising or lowering by several tenths, depending on the refractor velocity. Evidently there are other factors, such as radiation patterns and ground factors at the receiver, which contribute significantly to the data scatter. However, if we were to choose between the first computed value of 5.21 and the adjusted value of 4.73, we would favor 4.73 since P data were not observed beyond 86 degrees.

Generally, an "average" 5.2 event would generate diffracted P data which could easily be read on WWNSS seismograms.

SURFACE WAVE MAGNITUDES

The World-wide standard stations and the LRSM stations, which operate three-component long-period systems, provided the major source of the surface wave information. Data from other seismograph stations with similar instrumentation were used whenever possible.

Surface wave magnitudes were computed with the use of a formula

$$M_S = \log_{10} A/T + 1.66 \log_{10} \Delta^{\circ} + 3.3$$

where:

A = ground amplitude in microns

T = ground period in seconds

Δ = distance in degrees

developed by Vanek (1962) and adopted by the IASPEI Committee which recommended that the formula be applied to 20-sec waves. This was not possible in the case of GASBUGGY because the only observable waves had periods of circa 12 sec. A/T values measured from these waves were entered into the formula to obtain M_S. The Russians have indicated that the formula applies to other wave periods as well when the measurements of A/T are associated with maximum amplitudes (Soloviev and Shebalin, 1957; Gutenberg, 1945).

Based on the formula, the computed results from the three-component long-period seismographs are presented in Table 3.

The LRSM stations, as contrasted to the World-wide stations, recorded the larger surface wave periods. This factor could be related to the instrumental response resulting from the different galvanometers used in the seismograph system. Due to the sparse horizontal component magnitude data, only the LPZ component magnitude was graphically plotted.

The overall average magnitude (M_S) was 4.09 which was, as expected, lower than the average body wave magnitude (M_B) of 5.21 (Figure 14). Beyond 20 degrees, the surface wave magnitude was 4.53, approximately 0.5 of a magnitude unit lower than the computed body wave magnitude (M_B) for distances greater than 16 degrees. The characteristic pronounced shift of body wave magnitudes with increasing distance was not reflected by the surface wave magnitudes. The magnitude of the surface waves appeared to be more evenly distributed, although dispersed, throughout the distance range. As noted with body wave magnitudes beyond 16 degrees, there was a corresponding shift of surface wave magnitudes in the 17 degrees to 20 degrees distance range.

The surface wave magnitudes (Figure 14) do not appear to correlate with azimuth, wave period, or region. However, they do appear to be distance dependent, indicating a review of the attenuation function may be necessary.

Magnitudes calculated for GASBUGGY by long- and short-period instruments at the same station generally disagreed.

Figure 15 shows the M_S - M_B (observed at the same station) plotted versus distance, and Figure 16 exhibits similar pairs of M_S - M_E measurements. The relatively greater range of values shown in Figure 15 probably reflects the distance dependence of both M_S and M_B. The obvious improvement, when M_S and M_E are compared, indicates a fairly consistent relation between the two estimates of magnitude. In general, differences between the surface wave and body wave magnitudes decrease with increasing distance.

Figures 17 and 18 are plots of M_B vs M_S and M_E vs M_S, respectively, where each point refers to a pair of values at the same station. The straight line segments, which were developed by Gutenberg and Richter (1956), and by Romney (1963), represent the relationship between body and surface wave magnitudes of earthquakes. Again, more consistency is observed when M_E values are compared with M_S. Perhaps the most significant information which these last two graphs disclose is the high degree of scatter associated with pairs of magnitude values related to the same source, a simple compression, as compared at the same station.

A general comparison concerning M_B versus M_S shows that the relative excitation of long-period surface waves from explosions is less than that from shallow earthquakes since neither WWNSS, LRSM, nor Gutenberg and Richter (1956) curves appear to fit the GASBUGGY data.

A COMPARISON BETWEEN GASBUGGY AND AN EARTHQUAKE

On January 23, 1966 at 01h 56m 38s U.T., an earthquake occurred at 36.96°N and 106.90°W which placed the epicenter circa 40 kilometers northeast of the GASBUGGY test site. As both epicenters were essentially in the same place, an unusual opportunity was provided for a comparison of magnitudes, both M_B and M_S, from the two events.

The Gutenberg and Richter (1956) magnitude formula was used to compute the body wave magnitudes, whereas the surface wave magnitudes were computed by the formula given on page 14 in this report. Two procedures were used to obtain the average body and surface wave magnitudes for the two events: (1) total M_B and M_S magnitude data; (2) ten stations which recorded M_B and M_S magnitudes from GASBUGGY and from the earthquake. The total data resulted in an average M_B separation of 0.11 unit of magnitude between the two events [GASBUGGY: 5.21 (129 stations); Earthquake: 5.10 (34 stations)]. The average body wave magnitude for the ten-station network differed by only 0.20 unit (GASBUGGY 5.30; Earthquake 5.10).

The average surface wave magnitude for the total GASBUGGY data was 4.09 (42 stations) and for the earthquake the M_S was 5.42 (29 stations). This is a difference between body and surface wave magnitudes of 1.12 units for GASBUGGY and for the earthquake 0.32 unit. A comparison of the average surface wave magnitude for the ten stations shows 4.11 for GASBUGGY and 5.37 for the earthquake. The body minus

surface wave magnitude difference for GASBUGGY was 1.19 magnitude units as compared with the difference for the earthquake of 0.27 unit.

Figure 19 presents a plot of M_B versus M_S for the earthquake where each point refers to a pair of values at the same station. Particularly noticeable in Figure 19 is the apparent increase or decrease of M_S in relation to M_B as compared with Figure 17 at similar stations.

Figure 20 illustrates M_S - M_B measurements, which were observed at the same station, plotted versus distance for the earthquake. The majority of the earthquake data are positive which is in contrast to the negative values shown by the GASBUGGY data (Figure 15). The consistent relationship of the M_S - M_B values is noteworthy for similar stations, which recorded GASBUGGY and the earthquake, in the 4 degrees to 16 degrees distance range.

The difference in body and surface wave magnitude is one method of differentiating between a shallow earthquake and an explosion. It has been noted that if the difference is approximately one magnitude unit lower, an explosion source may be suspected. The significant difference between body and surface wave magnitudes, when GASBUGGY and the earthquake are compared, tends to lend validity to the earlier observation.

HYPOCENTER COMPUTATIONS

The results of the computer solutions which were carried out with the C&GS hypocenter program (Engdahl and Gunst, 1966), are shown in Table 4. The computations were performed with the use of the standard travel-time tables of Jeffreys-Bullen (1940) and the recently published Herrin tables (1968). The first line in Table 4 gives the known coordinates of the shot, and the remaining lines refer to computed solutions.

The results indicate that epicenters can be located within an accuracy of a few kilometers when the data include arrivals at local stations; i.e., observations of the "direct wave". The importance of having such nearby observations cannot be overstressed as they limit the error in location and are essential in fixing the depth of focus.

As has been noted previously (Carder, et. al., 1966), the Jeffreys-Bullen curve is a good first approximation of regional travel times in the Western mountain environment. An examination of residuals from all computations shows that, in general, they are azimuthally dependent, and that they indicate particularly poor agreement with the standard curves in the distance range of 10 to 20 degrees. This scatter is believed due to the observation that, depending on signal-to-noise conditions, the first identifiable arrival in this range may be associated with the $P_{7.9}$, $P_{8.5}$, or $P_{10.5}$ km/sec refractor.

Nearly all observations were late with respect to the 1968 curves, indicating velocities beneath the GASBUGGY site are relatively slow as has been suggested by Herrin and Taggart's (1968) seismic delay contours.

HYPOCENTER RELOCATION

An attempt to refine the computed hypocenter was also made by adjusting the GASBUGGY arrival times relative to the residuals observed from GNOME at 22 stations which recorded both events. The results were spurious. Using a restrained depth of 0 kilometers, the location was 36.738° N., 107.447° W., and a location representing unrestrained parameters was 36.720° N., 107.459° W. The shift of latitude and longitude toward the northwest, in kilometers, from the known coordinates was 6.66 north, 21.41 west, and for the latter solution, the shift was 4.66 north, 22.48 west. Apparently, at regional distances station corrections are dependent on azimuth and distance.

SUMMARY OF CONCLUSIONS

1. The recorded amplitudes of Pn and P at similar distances were equal, or the amplitudes were slightly higher to the west of GASBUGGY. Amplitudes of Pn and P appeared to be higher where the first arrival was early, and smaller where a late arrival was recorded.

2. The arrival times for all stations appeared to follow the Jeffreys-Bullen curve closely. The stations to the east of GASBUGGY were early, but not as early as found in GNOME. Stations to the west of GASBUGGY tended to be early, whereas GNOME showed more late arrivals. Beyond 20 degrees, the arrival times were about 1.0 sec earlier than the travel time predicted by the Jeffreys-Bullen table.

3. Arrival times and amplitudes of Pn and P appeared to be correlated with physiographic province.

4. Pg and Lg recorded amplitudes were higher to the east than to the west of GASBUGGY.

5. LQ waves were recorded to the east and to the west of GASBUGGY. The wave attenuation rate for the eastern stations appeared to be more rapid than for the stations to the west.

6. The overall average magnitude, when computed by the method given by Gutenberg and Richter (1956), was 5.21. Using the method suggested by Evernden (1967), an average magnitude was computed to be 4.73.

7. The recorded data confirm the Evernden (1967) apparent velocities, which indicate the absence of the $P_{7.9}$ velocity refractor beneath the Great Plains to the east. With the exception of two stations to the east, the arrival with the $P_{7.9}$ apparent velocity was not observed east of the Rocky Mountain Front.

8. Rayleigh waves were distinctly recorded at large distances from GASBUGGY, whereas GNOME recorded LR waves out to a distance of 500 kilometers. Twenty-second surface waves were not recorded from GASBUGGY. The surface wave magnitude (M_S) was 4.09 as compared with a M_B and M_E of 5.21 and 4.73, respectively. The observation that M_S is more than one magnitude unit less than M_B agrees with previously published results in discerning earthquakes from explosions.

9. The attempt to refine the GASBUGGY location, by correcting the arrival times relative to the observed residuals from GNOME, indicates that location accuracy is dependent on recording station distance and azimuthal control.

REFERENCES

Burke-Gaffney, T.N., Bullen, K.E., 1957, "Seismological and Related Aspects of the 1954 Hydrogen Bomb Explosions", Australian Journal of Physics, Vol. 10, pp. 130-136.

Carder, D.S, Bailey, L.F., 1958, "Seismic Wave Travel Times from Nuclear Explosions," B.S.S.A., Vol. 48, pp. 377-398.

Carder, D.S., Gordon, D.W., Jordan, J.N., 1966, "Analysis of Surface Focus Travel Times", B.S.S.A., Vol. 56, No. 4, pp. 815-840.

Coast and Geodetic Survey, 1968, "A Seismic Profile Southward from the GASBUGGY Explosion: Field Report," Geophysics Research Group and Seismology Division, Office of Seismology and Geomagnetism, ESSA, ARPA No. 1095.

Engdahl, E.R., Gunst, R.H., 1966, "Use of a High Speed Computer for the Preliminary Determination of Earthquake Hypocenters", B.S.S.A., Vol. 56, pp. 325-336.

Evernden, J.F., 1967, "Magnitude Determinations of Regional and Near Regional Distances in the United States", B.S.S.A., Vol. 57, pp. 591-637.

Geotech, 1967, "Long Range Seismic Measurements-GASBUGGY," ARPA Project No. VT/8703, Garland, Texas, A Teledyne Company.

Gevertz, H., Lemon, R.F., Hollis, W.T., (EPNG), Lekas, M.A., (AEC), Ward, D.C., Atkinson, C.H., (USBM), and Dr. Bonner, D., (LRL), "Project GASBUGGY", May 14, 1965.

Gutenberg, B., 1945, "Amplitudes of Surface Waves and Magnitudes of Shallow Earthquakes", B.S.S.A., Vol. 35, pp. 3-12.

Gutenberg, B., Richter, C.F., 1956, "Magnitude and Energy of Earthquakes," Annali di Geofisica, Vol. IX, pp. 1-15.

Gutenberg, B., Richter, C.F., 1964, "Seismic Waves from Atom Bomb Test," Translations, American Geophysical Union, Vol. 27, p. 776.

Herrin, E., Minton, P.D., 1960, "The Velocity of Lg in the Southwestern United States and Mexico", B.S.S.A., Vol. 50, pp. 35-44.

Herrin, E., Taggart, J., 1963, "The Use of Calibration Shots in the Determination of Hypocenters," ARPA Air Force Grant No. AFOSR-61-137.

Herrin, E., Taggart, J., 1968, "Regional Variations in P Travel Times," B.S.S.A., Vol. 58, No. 4, pp. 1325-1337.

Jeffreys, H., Bullen, K.E., 1940, "Seismological Tables," British Association for the Advancement of Science, Gray Milne Trust.

Jordan, J.N., Black, R., Bates, C.C., 1965, "Patterns of Maximum Amplitudes of Pn and P Waves over Regional and Continental Areas," B.S.S.A., Vol. 55, No. 4, pp. 693-720.

Kelley, V.C., 1955, "Regional Tectonics at the Colorado Plateau and Relationship to the Origin and Distribution of Uranium," University of New Mexico, Publications on Geology, No. 5.

Mickey, W.V., Devine, J.F., Meyer, A.V.C., 1968, "Project GASBUGGY, Response of the Mesita de Los Alamos to the GASBUGGY Experiment and Induced Vibrations," C&GS Seismology Division, Unpublished.

Romney, C., Brooks, B.G., Mansfield, R.H., Carder, D.S., Jordan, J.N., Gordon, D.W., 1962, "Travel Times and Amplitudes of Principal Body Phases Recorded from GNOME," B.S.S.A., Vol. 52, No. 5, pp. 1057-1074.

Romney, C., 1963, "An Investigation of the Relationship Between Magnitude Scales for Small Shocks", AFTAC Technical Report, VU-63-4, Project Vela Uniform.

Soloviev, S.L., Shebalin, N.V., 1957, "Determining the Intensity of an Earthquake from the Surface Wave Ground Displacement," Izv. Akad. Nauk. SSSR., Ser. Geofiz., No. 7, pp. 926-930.

Stauder, W., S.J., 1964, "A Review of Russian Work in Magnitude Determination," Proceeding of the VESIAC Conference on Seismic Event Magnitude Determination, pp. 13-34.

Vanek, J., Zatopek, A., et. al., 1962, "Standardization of Magnitude Scales," Izv. Akad. Nauk. SSSR., Ser. Geofiz., No. 2, pp. 153-158.

TABLE 1. -- GASBUGGY Event, Arrival Times and Amplitudes of Principal Phases

CODE	Station	Distance Degrees	Distance km	Com-ponent	Phase	Obs. Arrival Time** 1900 Hrs. Min.	Sec.	Period T Sec.	Maximum Amplitude A/T (mμ/sec)	Magnitude M_B	M_E	J.B. Residual	Remarks
IR1	Lindrith New Mexico	0.39	44	SPZ Lo	iPgc	30	08.8					0.8	
				SPZ Lo	eP*	30	10.4						
				SPT Hi	eS*	30	21.8						
IR2	Cuba New Mexico	0.69	78	SPZ Hi	ePg	30	14.4					0.3	
				SPZ Hi	eP*	30	15.0						
				SPZ Hi	e(Pn)	30	16.5						
				SPT Lo	eSg	30	17.7						
				SPR Lo	eS*	30	20.7						
				SPT Lo	eS*	30	20.7						
IR3	San Luis New Mexico	1.01	111	SPZ Hi	iPgc	30	19.3	0.3	23000.0			-0.9	
				SPZ Hi	eP*	30	20.7	0.1	74600.0				
				SPZ Hi	ePn	30	21.2	0.2	41200.0				
				SPE Hi	eSg	30	31.0	0.3	51387.0				
				SPN Hi	eSg	30	31.0	0.2	50000.0				
IR4	Puerco Dam New Mexico	1.36	156	SPZ Hi	iPc	30	25.0	0.2	22500.0			-1.3	Instrument Damage No field cali-bration
				SPZ Hi	ePg	30	27.5	0.2	49375.0				
				SPE Hi	eLg(S*)	30	42.5	0.4	9630.0				
				SPN Hi	eLg(S*)	30	42.5	0.3	35293.0				
R15	Taos New Mexico	1.37	156	SPZ Hi	ePg	30	25.0	0.2	4725.0			-0.4	
				SPZ Hi	ePn	30	26.9	0.3	8590.0				
				SPZ Hi	eP*	30	27.4	0.35	10400.0				
				SPN Hi	eSg	30	41.9	0.25	5800.0				
				SPE Hi	eSg	30	41.9	0.4	2812.0				

**Uncorrected for ellipticity and station elevation

CODE	Station	Distance Degrees	Distance km	Com-ponent	Phase	Obs. Arrival Time 1900 Hrs. Min.	Obs. Arrival Time 1900 Hrs. Sec.	Period T Sec.	Maximum Amplitude A/T (mμ/sec)	Magnitude M_B	Magnitude M_g	J.B. Residual	Remarks
IR5	Mesa Blanca New Mexico	1.52	167	SPZ Hi	iPnc	30	29.0	0.2	18750.0			0.2	
				SPZ Hi	eP*	30	29.8	0.4	22325.0				
				SPZ Hi	ePg	30	31.0	0.3	28307.0				
				SPE Hi	eLg(Sn)	40	46.7	0.4	20250.0				
				SPN Hi	eLg(Sn)	40	46.7	0.3	19866.0				
ALQ	Albuquerque New Mexico	1.84	205	SPZ	iPc	30	33.4	0.5	6674.0			0.0	
				SPN	i(S)	30	51.0	0.8	730.0				
				SPE	i(S)	30	51.0	0.8	696.0				
				SPN	iL	31	00.5	0.6	1145.0				
				SPE	iL	31	00.5	0.9	1852.0				
IR6	South Garcia New Mexico	1.80	200	SPZ Hi	iP*c	30	33.6	0.4	1680.0			0.8	SPE inoperative
				SPZ Lo	ePg	30	35.1						Low gain Z trace inoperative Data not reliable
				SPN Lo	Lg(Sn)	30	56.5	0.4	6425.0				
R16	Mora Ranch New Mexico	1.92	211	SPZ Hi	e(Pn)	30	35.6					0.9	No amplitude or period for Pn
				SPZ Lo	e(P*)	30	36.3	0.4	5350.0				
				SPN Lo	eLg	30	36.4	0.3	853.0				
				SPE Lo	eLg	30	36.4	0.2	945.0				
IR7	Mesa Aparejo New Mexico	2.00	222	SPZ Hi	iPnc	30	36.1	0.3	1670.0	(5.4)	5.4	0.4	
				SPZ Lo	eP*	30	37.2	0.25	9199.0				
				SPZ Lo	ePg	30	40.0	0.3	9270.0				
				SPN Lo	eLg(Sn)	31	01.5	0.4	8320.0				
				SPE Lo	eLg(Sn)	31	01.5	0.3	2000.0				

CODE	Station	Distance Degrees	Distance km	Com-ponent	Phase	Obs. Arrival Time 1900 Hrs. Min.	Obs. Arrival Time 1900 Hrs. Sec.	Period T Sec.	Maximum Amplitude A/T (mμ/sec)	Magnitude MB	Magnitude MS	J.B. Residual	Remarks
IR8	Ladron Mountain New Mexico	2.22	244	SPZ Hi	eP	30	38.9	0.2	1060.0	5.5	4.7	0.0	
				SPZ Lo	eP*	30	41.8	0.2	3620.0				
				SPZ Lo	ePg	30	43.1	0.2	1945.0				
				SPN Lo	eLg	31	08.6	0.3	2680.0				
				SPE Lo	eLg	31	08.6	0.35	1280.0				
SNM	Socorro New Mexico	2.61	289	SPZ Hi	iPg	30	44.2	0.3	134.0	4.6	4.0	-0.3	No horizontals
				SPZ Lo	eP*	30	47.7	0.3	3200.0				
R11	Bear Den School New Mexico	3.33	367	SPZ Hi	eP	30	54.1	0.3	83.3	4.8	4.1	-0.6	
				SPZ Hi	e(P*)	30	57.5	0.2	319.0				
				SPZ Hi	e(Pg)	31	00.4	0.2	845.0				
				SPN Lo	eLg	31	35.0	0.3	302.6				
				SPE Lo	eLg	31	35.0	0.3	302.6				
GOL	Golden Colorado	3.35	389	SPZ	iPnc	30	55.4	0.5	553.0	5.7	4.8	0.4	
				SPZ	iPg	31	02.1	0.7	584.0				
				SPZ	e(Sn)	31	34.4	(1.0)	(184.0)				
				LPZ	LR	32	00.0	8.0	389.0				
DEN	Denver Colorado	3.55	400	SPZ	ePn	30	58.3	(1.2)	150.0	5.1	4.4	0.5	
				SPZ	ePg	31	05.7	(1.0)	1810.0				
				SPN	eSn	31	35.5	1.4	775.0				
				SPN	eLg	31	53.8	1.4	757.0				
				SPE	eLg	31	55.0	1.3	1495.0				No response curve
				LPZ	LR	32	07.3						

CODE	Station	Distance Degrees	Distance km	Com-ponent	Phase	Obs. Arrival Time 1900 Hrs. Min.	Sec.	Period T Sec.	Maximum Amplitude A/T (mμ/sec)	Magnitude MB	ME	J.B. Residual	Remarks
GCA	Glen Canyon Arizona	3.53	389	SPZ	iPnc	30	58.5					1.2	clipped
PMC	Poorman Mine Colorado	3.66	411	SPZ SPZ	iPnc ePg	31 31	00.9 09.2	0.4	362.5	5.6	4.8	0.8	Letter report No period and amplitude given
BOU	Boulder Colorado	3.66	411	SPZ	iPnc	31	00.3	0.4	412.5	5.6	4.8	1.0	Letter report
R12	Hembrillo New Mexico	3.81	422	SPZ Hi SPZ Hi	eP eP*	31 31	00.8 08.1	0.35 0.3	26.0 440.0	4.5	3.6	-0.7	Lg clipped, Lo gain inoperative
HCU	Horse Canyon Utah	3.74	411	SPZ	iPo	31	01.0					0.4	clipped
FLA	Flats Utah	3.78	422	SPZ	iPc	31	01.0					0.2	clipped
SCU	Sheep Canyon Utah	3.69	411	SPZ	iPc	31	02.1					2.5	clipped
PCU	Price Utah	4.08	454	SPZ SPZ SPN SPE	iPc ePg eLg eLg	31 31 32 32	05.5 16.3 20.0 20.0	(0.9) 0.9 1.5 1.5	417.0 506.0 1043.0 1525.0	5.7	4.0	0.3	

CODE	Station	Distance Degrees	km	Com-ponent	Phase	Obs. Arrival Time 1900 Hrs. Min.	Sec.	Period T Sec.	Maximum Amplitude A/T (mμ/sec)	Magnitude M_B	M_E	J.B. Residual	Remarks
*TFO	Tonto Forest	4.08	454	SPZ	ePn	31	05.6	0.4	1951.8	6.4	5.3	0.4	
	Observatory			SPZ	ePg	31	15.3	0.4	3411.0				
	Arizona			SPE	eLg	32	03.0	0.4	3170.5				
*UBO	Uinta Basin	4.08	454	SPZ	ePn	31	06.1	0.4	483.2	5.8	5.1	0.9	
	Observatory			SPZ	ePg	31	16.1	0.5	2272.5				
	Utah			SPN	eLg	32	04.	0.4	795.9				
				LPE	LQ	32	17.	14.0	319.9				
				LPZ	LR	32	29.	16.0	485.4				
*LC-NM	Las Cruces	4.30	478	SPZ	ePn	31	07.5	0.2	128.4	5.3	4.8	-0.8	
	New Mexico			SPZ	ePg	31	19.2	0.6	676.9				
				SPR	eLg	32	14.	C.5	562.4				
				LPT	LQ	32	22.	13.0	78.0				
				LPZ	LR	32	37.	13.0	136.8				
*KN-UT	Kanab	4.52	503	SPZ	ePn	31	11.8	0.4	858.2	6.2	5.1	0.3	
	Utah			SPZ	ePg	31	27.0						Clipped
				SPT	eLg	32	23.						Clipped
				LPT	LQ	32	24.	13.5	99.9				
				LPZ	LR	32	38.	13.0	256.7				
FGU	Flaming Gorge	4.57	511	SPZ	iPc	31	12.7					0.3	Clipped
	Utah			SPE	eLg	31	24.6						Clipped
EPT	El Paso	4.93	544	SPZ	e(P)	31	14.5					-2.9	Periods & amplitude
	Texas			SPZ	eP*	31	21.5						not readable
				SPZ	ePg	31	29.5						No Horizontals

Code	Station	Distance Degrees	Distance km	Com-ponent	Phase	Obs. Arrival Time 1900 Hrs. Min.	Sec.	Period T Sec.	Maximum Amplitude A/T (mμ/sec)	Magnitude M_b	Magnitude M_s	J.B. Residual	Remarks
MMA	Mummy Mountain Arizona	4.99	555	SPZ	iP	31	16.5					-1.6	Telegraphic report
TUC	Tucson Arizona	5.26	589	SPZ	ePn	31	19.8	0.6	33.9	5.0	4.4	-2.3	
				SPZ	ePg	31	37.4						Clipped
				LPE	LQ	32	46.	10.0	74.1				
				LPZ	LR	33	20.	8.0	313.0				
LUB	Lubbock Texas	5.36	600	SPZ	eP	31	23.0					-0.3	Telegraphic report
				SPZ	e(Pg)	31	37.0						
SLC	Salt Lake City Utah	5.46	611	SPZ	e(Pn)	31	24.6	1.2	8.9	4.8	3.8	-0.3	
				SPZ	e(P*)	31	33.6	1.0	109.0				
				SPZ	iPg	31	41.6	1.1	604.5				
				SPE	eLg	32	59.0	6.0	329.0				
DUG	Dugway Utah	5.63	622	SPZ	ePn	31	24.7	0.8	125.0	5.2	5.0	-2.6	
				SPZ	eP*	31	31.5	0.5	382.0				
				SPZ	ePg	31	44.5	0.9	583.0				
				SPN	eLg	32	50.9	0.65	267.0				
				LPN	LQ	32	58.	3.5	226.0				
				LPZ	LR	33	28.	10.0	315.0				
*CQ-NV	Caliente Nevada	5.92	658	SPZ	ePn	31	29.0	0.5	28.4	4.9	4.5	-2.3	
				SPZ	ePg	31	52.6	0.5	632.9				
				SPT	eLg	33	05.	0.6	487.5				
				LPT	LQ	33	16.	11.0	144.4				
				LPZ	LR	33	34.	14.0	208.5				

CODE	Station	Distance Degrees	Distance km	Component	Phase	Obs. Arrival Time 1900 Hrs. Min.	Obs. Arrival Time 1900 Hrs. Sec.	Period T Sec.	Maximum Amplitude A/T (mμ/sec)	Magnitude M_b	Magnitude M_s	J.B. Residual	Remarks
LOG	Logan Utah	6.19	689	SPZ	iPn	31	34.2	1.6	119.0	5.7	5.2	-1.0	
				SPZ	ePg	31	59.1	1.6	472.0				
				WAN	eLg	33	15.	1.5	300.0				Wood-Anderson Horizontal
BCN	Boulder City Nevada	6.20	689	SPZ	iPn	31	34.5	0.9	64.9	5.3	4.9	-0.7	
				SPZ	eP*	31	47.1	(0.7)	121.0				
				SPZ	iPg	31	54.9					•	Unable to read period and amplitude-light trace
*PQ-ID	Preston Idaho	6.55	728	SPZ	ePn	31	38.6	0.5	43.6	5.4	4.8	-1.5	
				SPZ	ePg	32	01.4						Clipped
				SPR	eLg	33	19.	0.6	300.6				
				LPT	LQ	33	39.	16.0	50.9				
				LPZ	LR	33	58.	15.0	158.4				
*TL-WY	Thermopolis Wyoming	6.87	764	SPZ	ePn	31	42.5	0.4	90.5	5.9	4.4	-2.2	
				SPZ	ePg	32	03.5	1.0	536.8				
				SPT	eLg	33	27.	1.0	279.5				
				LPT	LQ	33	45.	16.5	63.9				
				LPZ	LR	34	16.	16.3	57.9				
LVN	Las Vegas Nevada	6.42	711	SPZ	eP	31	48.0					9.6	Telegraphic report
GLA	Glamis California	7.23	800	SPZ	iP	31	48.7					-1.0	Telegraphic report

CODE	Station	Distance Degrees	km	Com-ponent	Phase	Obs. Arrival Time 1900 Hrs. Min.	Sec.	Period T Sec.	Maximum Amplitude A/T (mμ/sec)	Magnitude M_B	M_R	J.B. Residual	Remarks
*WMSO	Wichita Mountain Observatory Oklahoma	7.28	810	SPZ	ePn	31	48.7	0.3	17.9	5.3	4.6	-1.6	
				SPZ	ePg	32	12.7	0.5	603.2				
				LPE	LQ	33	49.	28.0	5.8				
				LPZ	LR	33	57.	12.0	350.1				
EUR	Eureka Nevada	7.46	833	SPZ	iPn	31	51.7	(0.8)	204.0	6.3	4.9	-1.4	
*WZ-NV	Warm Springs Nevada	7.48	832	SPZ	ePn	31	52.0	0.5	9.9	5.0	4.3	-1.3	
				SPZ	ePg	32	18.4	0.7	302.7				
				SPT	eLg	33	52.	0.7	182.2				
				LPT	LQ	34	05.	12.0	97.9				
				LPZ	LR	34	35.	14.0	226.7				
GSC	Gold Stone California	7.90	878	SPZ	iP	31	58.0					-1.1	Telegraphic report
				SPZ	iPg	32	29.2						
TNF	Tonopah Nevada	8.09	900	SPZ	ePn	31	59.4	0.5	36.7	5.6	4.2	-2.5	
				SPZ	ePP	32	08.9	0.6	83.3				
				SPZ	ePg	32	31.4	1.0	317.0				Lg masked by noisy trace
				LPN	LQ	34	33.	9.0					
				LPZ	LR	35	03.	11.0					No LP curve
RCD	Rapid City South Dakota	7.99	889	SPZ	eP	32	00.1	1.1	26.2	5.5	4.1	-0.3	
				SPZ	ePP	32	11.8	0.6	72.9				
				SPZ	ePg	32	29.0	1.0	154.0				
				SPN	eLg	36	03.8	1.0	158.0				
				SPE	eLg	36	03.8	1.0	24.4				
				LPZ	LR	34	51.	8.0	83.6				

CODE	Station	Distance Degrees	Distance km	Component	Phase	Obs. Arrival Time 1900 Hrs. Min.	Obs. Arrival Time 1900 Hrs. Sec.	Period T Sec.	Maximum Amplitude A/T (mμ/sec)	Magnitude M_B	Magnitude M_S	J.B. Residual	Remarks
CLC	China Lake California	8.44	933	SPZ	iP	32	05.2					-1.4	Telegraphic report
*WN-SD	Winner South Dakota	8.49	944	SPZ	ePn	32	05.4	0.6	156.4	6.3	4.9	-1.8	
				SPZ	e(PP)	32	15.0	0.5	471.3				
				SPZ	ePg	32	37.4	0.5	864.1				
				SPT	eLg	34	36.	0.6	581.8				
				LPR	LQ	34	27.	12.0	95.2				
				LPZ	LR	35	13.	12.0	151.4				
PLM	Palomar California	8.58	956	SPZ	iP	32	07.5					-1.3	Telegraphic report
MHT	Manhattan Kansas	8.77	978	SPZ	ePn	32	08.7	0.5	135.2	6.3	4.8	-2.4	
				SPZ	e(PP)	32	18.5	0.6	126.5				
				SPZ	ePg	32	41.3	(1.0)	526.0				
				SPN	eLg	34	38.	1.3	166.0				
				SPE	eLg	34	42.	1.1	810.0				
*MN-NV	Mina Nevada	8.86	986	SPZ	ePn	32	09.8	0.5	4.9	4.9	4.3	-2.7	
				SPZ	ePg	32	41.2	0.8	56.3				
				SPR	eLg	34	45.	0.8	58.5				
				LPT	LQ	34	47.	12.5	64.2				
				LPZ	LR	35	05.	13.0	242.0				
RVR	Riverside California	8.73	967	SPZ	iP	32	10.0					-0.6	Telegraphic report
CWC	Cottonwood California	8.75	978	SPZ	iP	32	10.7					-0.4	Telegraphic report

CODE	Station	Distance Degrees	km	Com-ponent	Phase	Obs. Arrival Time 1900 Hrs. Min.	Sec.	Period T Sec.	Maximum Amplitude A/T (mμ/sec)	Magnitude M_B	M_R	J.B. Residual	Remarks
*HL2ID	Hailey Idaho	8.82	980	SPZ	ePn	32	10.8	0.5	12.6	5.3	4.6	-1.0	
				SPZ	e(PP)	32	22.9	0.9	33.5				
				SPZ	ePg	32	39.7	0.7	36.4				
				SPT	eLg	34	31.	1.0	24.1				
				LPR	LQ	34	50.	14.0	28.2				
				LPZ	LR	34	57.	13.0	227.9				
*GV-TX	Grapevine Texas	9.21	1024	SPZ	ePn	32	14.5	0.5	3.2	4.7	4.1	-2.6	
				SPZ	e(PP)	32	22.6	0.6	15.5				
				SPZ	ePg	32	50.6	0.5	161.7				
				SPZ	eLg	34	45.	1.0	64.1				
*BS-MA	Billings Montana	9.13	1016	SPZ	ePn	32	14.7	0.4	35.5	5.8	4.3	-1.4	
				SPZ	ePg	32	51.0	1.0	155.3				
				SPR	eLg	34	49.	1.0	84.7				
				LPZ	LR	35	19.	15.0	79.0				
ISA	Isabella California	9.17	1022	SPZ	iP	32	15.8					-1.0	Telegraphic report
				SPZ	iPg	32	49.2						
LF3	Lasa F-Ring Montana	9.29	1033	SPZ	iP	32	16.3	1.0	14.2	5.4	4.7	-2.0	Telegraphic report
TUL	Tulsa Oklahoma	9.25	1027	SPZ	e(P)	32	18.0					0.2	Noisy
				SPZ	iPg	32	23.8	0.6	102.5				
				SPZ	ePP	32	50.7	1.0	86.9				
				SPZ	eLg	34	53.5	0.9	222.0				

CODE	Station	Distance Degrees	km	Com-ponent	Phase	Obs. Arrival Time 1900 Hrs. Min.	Sec.	Period T Sec.	Maximum Amplitude A/T (mμ/sec)	Magnitude M_B	M_R	J.B. Residual	Remarks
UVN	Unionville	9.36	1038	SPZ	ePn	32	18.3	0.5	15.7	5.4	4.0	-1.3	
	Nevada			SPZ	ePg	33	57.5	0.7	61.3				
				SPZ	iLg	34	58.5	2.5	117.5				
PAS	Pasadena	9.30	1033	SPZ	iP	32	18.4					0.0	Telegraphic report
	California			SPZ	iPg	32	52.4						
					iLg	34	48.4						
BOZ	Bozeman	9.52	1056	SPZ	ePn	32	20.3	0.8	7.3	5.1	4.5	-1.3	
	Montana			SPZ	e(P*)	32	22.9	0.6	31.4				
				SPZ	ePg	33	03.5	1.0	37.5				
				SPN	eLg	35	07.0	1.4	25.0				
				SPE	eLg	35	07.0	1.5	20.0				
BZM	Bozeman	9.43	1048	SPZ	ePn	32	21.0	1.3	8.7	5.2	4.6	0.6	
	Montana			SPZ	ePg	33	30.0	1.0	13.5				
LAW	Lawrence	9.73	1078	SPZ	ePn	32	22.0	1.2	38.1	5.9	4.4	-2.4	
	Kansas			SPZ	ePg	33	03.0	0.9	338.0				
				SPN	eLg	35	04.4	1.2	134.0				
				SPE	eLg	35	04.4	1.3	210.0				
*LAO	Subarray AO-10	10.03	1115	SPZ	ePn	32	25.6	0.5	46.6	6.0	4.5	-2.8	
	Montana			SPZ	ePg	33	12.4	0.7	72.9				
				D3-EHi	LQ	35	33.	12.0	(5.15)				
				D3-ZHi	LR	35	52.	16.0	32.7				

CODE	Station	Distance Degrees	km	Component	Phase	Obs. Arrival Time 1900 Hrs. Min.	Sec.	Period T Sec.	Maximum Amplitude A/T (mμ/sec)	Magnitude M_B	M_R	J.B. Residual	Remarks
BUT	Butte Montana	10.16	1133	SPZ	eP	32	29.6	(0.9)	(50.0)	6.0	4.5	-0.8	
				SPZ	ePP	32	40.5	1.0	102.0				
				SPZ	ePg	33	13.7	(0.9)	61.1				
REN	Reno Nevada	10.37	1156	WAE	eLg	32	46.	2.5	360.0				No SPZ Inst.
				WAN	eLg	32	46.	2.0	500.0				Wood Anderson
				LPZ	LR	36	26.	11.0	256.0				Horizontals
NRR	North Reno Nevada	10.37	1156	SPN	eLg	35	24.	3.0	145.0				No SPZ Inst.
FAY	Fayetteville Arkansas	10.51	1167	SPZ	ePn	32	32.3	0.7	17.7	6.5	4.1	-2.9	
				SPZ	ePg	33	13.8	0.5	754.0				
				SPZ	eLg	35	38.9	1.0	935.0				
				LPN	(LQ)	35		4.8	40.2				
*LN-MA	Lewistown Montana	10.62	1178	SPZ	ePn	32	34.2	0.6	28.3	5.7	4.3	-2.5	
				SPZ	ePg	33	34.3	0.9	46.3				
				SPT	eLg.	35	29.	0.9	29.1				
				LPT	LQ	35	50.	17.0	31.7				
				LPZ	LR	36	24.	15.0	58.4				
JAS	Jamestown California	10.62	1178	SPZ	ePn	32	35.9	0.7	7.4	5.1	4.7	-0.7	
				SPZ	ePg	33	16.5	1.0	16.5				
				SPN	eLg	35	34.	2.5	101.0				
				SPE	eLg	35	37.	2.5	520.0				

CODE	Station	Distance Degrees	Distance km	Com-ponent	Phase	Obs. Arrival Time 1900 Hrs. Min.	Obs. Arrival Time 1900 Hrs. Sec.	Period T Sec.	Maximum Amplitude A/T (mμ/sec)	Magnitude M_B	Magnitude M_F	J.B. Residual	Remarks
SYP	Santa Ynez Peak California	10.62	1178	SPZ	iP	32	37.3					0.6	Telegraphic report
PRI	Priest California	10.86	1211	SPZ	e(P)	32	43.3					3.3	Too emergent for accurate period & amplitude measurements
				SPZ	e(Pg)	33	30.1	1.7	17.0				
				SPZ	eLg	35	44.7	2.5	417.0				
BMO	Blue Mountain Observatory Oregon	11.18	1242	SPZ	eP	32	43.9	0.75	50.0	5.1	4.7	-0.5	
				SPZ	ePP	32	55.0	0.7	38.6				
				SPZ	ePg	33	34.0	0.6	49.0				
				SPE	eLg	35	49.6	1.4	31.5				
				SPN	eLg	35	49.6	1.7	28.4				
SLD	San Luis Dam California	11.23	1245	SPZ	ePn	32	47.4	0.6	19.3	4.6	4.2	2.4	
				SPZ	ePP	33	06.3	1.2	6.1				
				SPZ	ePg	33	28.9	1.1	16.4				
				SPN	eLg	36	53.	1.8	3.1				
				SPE	eLg	36	53.	1.4	4.3				
MHC	Mt. Hamilton California	11.56	1284	SPZ	e(P)	32	47.4	(1.0)	(7.4)	(5.0)	3.8	-2.2	
				SPZ	ePg	33	41.7	0.9	8.1				
				SPZ	eLg	36	08.	2.0	8.1				
ORV	Oroville California	11.62	1290	SPZ	eP	32	50.7					0.4	Telegraphic report
				---	eLg	36	13.5						

CODE	Station	Distance Degrees	km	Com-ponent	Phase	Obs. Arrival Time 1900 Hrs. Min.	Sec.	Period T Sec.	Maximum Amplitude A/T (mμ/sec)	Magnitude Mb	Ms	J.B. Residual	Remarks
*HV-MA	Havre Montana	11.89	1323	SPZ	ePn	32	51.0	0.6	33.3	5.6	4.4	-2.9	
				SPZ	e(PP)	33	00.4	0.6	23.9				
				SPZ	ePg	33	37.5	1.1	50.0				
				SPR	eLg	36	24.	1.1	44.4				
				LPR	LQ	36	07.	22.0	26.7				
				LPZ	LR	37	16.	15.0	60.1				
MIN	Mineral California	11.86	1322	SPZ	e(P)	32	51.8	0.6	14.4	5.3	4.1	-1.8	
				SPZ	ePP	33	02.2	0.6	44.6				
				SPZ	eLg	36	17.6	(0.3)	(111.0)				
STC	Stone Canyon California	11.27	1256	SPZ	e(P)	32	(57.)	1.6	36.4			11.5	
*PH-WA	Pomeroy Washington	12.35	1363	SPZ	ePn	32	58.5	0.8	23.9	5.5	4.3	-0.2	
				SPZ	ePP	33	17.7	1.0	55.4				
				SPZ	ePg	33	35.3	0.9	23.0				
				SPT	eLg	36	43.	1.2	20.7				
				LPT	LQ	36	44.	14.0	58.9				
				LPZ	LR	37	26.	15.0	123.1				
SLM	St. Louis Missouri	13.59	1511	SPZ	eP	33	12.9	0.6	362.0	6.3	5.6	-3.7	
				SPZ	ePP	33	25.6	0.6	708.3				
				SPZ	ePg	34	10.8	0.9	915.0				
				SPN	eLg	37	15.5	0.9	76.4				
				SPE	eLg	37	17.5	1.1	79.5				
				LPZ	LR	38	18.	8.0					No LP curve
SAO	San Andreas Geophysical Obs. California			SPN	eLg	36	08.	(2.3)	81.0				

CODE	Station	Distance Degrees	Distance km	Com-ponent	Phase	Obs. Arrival Time 1900 Hrs. Min.	Obs. Arrival Time 1900 Hrs. Sec.	Period T Sec.	Maximum Amplitude A/T (mμ/sec)	Magnitude M_b	Magnitude M_s	J.B. Residual	Remarks
SPO	Spokane Washington	13.34	1484	SPN	eP	33	13.7	0.8	8.9			0.4	SPZ Noisy and underdamped very weak Lg
				SPN	eLg								
NEW	Newport Washington	13.68	1522	SPZ	eP	33	17.0	0.9	30.9	5.2	4.6	-0.8	
				SPZ	ePP	33	26.5	1.0	149.0				
				LPZ	LR	38	40.	11.0	32.4				
DBQ	Dubuque Iowa	14.00	1556	SPZ	eP	33	19.8	0.6	33.2	5.1	4.6	-2.2	
				SPZ	ePP	33	21.7	0.7	53.7				
				SPZ	ePg	34	20.9	0.8	139.0				
				SPZ	eLg	37	39.5	0.9	136.0				
				LPZ	LR	39	18.	6.0	0.76				underdamped
SES	Suffield Canada	13.99	1556	SPZ	eP	33	21.0	0.5	3.5	4.1	3.6	-0.8	
				SPZ	ePg	34	24.5	1.1	102.0				
				SPN	eLg	37	46.	1.3	42.4				
				SPE	eLg	37	46.	1.2	58.4				
				LPZ	LR	38	36.	12.0	3.52				
NTI	Nordman Idaho	13.92	1544	SPZ	eP	33	21.5	0.8	37.5	5.2	4.7	0.6	
				SPZ	ePP	33	29.5	1.2	93.0				
OXF	Oxford Mississippi	14.65	1627	SPZ	eP	33	26.4	1.4	190.0	5.8	4.7	-4.1	
				SPZ	ePP	33	38.0	0.9	83.4				
				SPZ	ePg	34	33.9	1.1	222.0				
				SPE	eLg	37	20.	1.2	101.8				
				SPN	eLg	37	20.	1.5	86.7				
				LPZ	LR	38	56.	10.0	43.5				

CODE	Station	Distance Degrees	Distance km	Com-ponent	Phase	Obs. Arrival Time 1900 Hrs. Min.	Sec.	Period T Sec.	Maximum Amplitude A/T (mμ/sec)	Magnitude M_b	M_s	J. B. Residual	Remarks
*CC-WA	Cascade Tunnel	15.09	1678	SPZ	eP	33	36.6	1.0	4.3	3.9	3.8	0.4	
	Washington			LPZ	LR	39	20.	16.0	42.2				
LON	Longmire	14.81	1644	SPZ	eP	33	36.8	1.0	12.5	4.5	4.2	4.1	
	Washington												
PNT	Penticton	15.53	1722	SPZ	eP	33	41.4	1.2	167.0	5.3	4.8	-0.5	
	Canada			SPZ	ePP	33	56.4	1.3	56.5				
				SPE	(eLg)	38	45.	1.5	60.0				
				LPZ	LR	39	45.	10.5	144.0				
TUM	Tumwater	15.58	1733	SPZ	e(P)	33	40.5	1.0	71.4	4.9	5.0	-2.0	
	Washington												
BLO	Bloomington	16.51	1833	SPZ	iPc	33	51.7	1.2	62.5	4.7	5.1	-2.9	
	Iowa			SPN	eLg	38	45.	1.1	160.0				
				SPE	eLg	38	45.	1.0	185.0				Underdamped
				LPZ	LR	39	56.7	9.0					No LP curve
*LY-WA	Lynden	16.23	1805	SPZ	eP	33	51.6	0.9	66.5	4.7	4.4	0.7	
	Washington			LPZ	LR	39	43.	17.0	83.5				
*RK-ON	Red Lake	17.16	1908	SPZ	eP	33	58.6	0.6	9.1	3.9	4.3	-4.0	
	Ontario, Canada			SPT	eLg	38	13.	1.1	64.5				
				LPT	LQ	39	08.	12.0	32.6				
				LPZ	LR	40	03.	15.0	29.3				

CODE	Station	Distance Degrees	km	Com-ponent	Phase	Obs. Arrival Time 1900 Hrs. Min.	Sec.	Period T Sec.	Maximum Amplitude A/T (mμ/sec)	Magnitude M_B	M_S	J.B. Residual	Remarks
EDM	Edmonton Canada	17.09	1900	SPZ	eP	34	00.7	1.1	166.0	5.1	5.0	-1.2	
				SPZ	ePP	34	18.4	1.2	25.0				
				SPN	eLg	39	40.	1.1	28.6				
				SPE	eLg	39	40.	1.0	35.8				
CPO	Cumberland Plateau Tennessee	17.51	1944	SPZ	eP	34	06.4	0.8	11.8	4.2	4.4	-0.9	
				SPZ	ePP	34	17.4	0.7	71.5				
				SPE	eLg	38	53.	1.1	83.0				
				SPN	eLg								Unable to distinguish between traces.
				LPZ	LR	39	20.	17.0	173.4				
FFC	Flin Flon Canada	18.41	2044	SPZ	eP	34	16.2	1.3	176.0	4.2	5.1	-2.1	
				SPN	eLg	40	23.0	1.1	8.1				
				SPE	eLg	40	23.0	1.8	52.6				
CNN	Cincinnati Ohio	18.08	2011	SPZ	e(P)	34	16.5					2.1	Noisy. Unable to read period and amplitude
ORT	Oak Ridge Tennessee	18.47	2056	SPZ	iP	34	17.0					-2.1	Telegraphic report
				---	eLg	39	17.0						
AAM	Ann Arbor Michigan	19.00	2111	SPZ	eP	34	23.7	0.5	64.0	4.8	5.7	-1.9	
				SPZ	e(PP)	34	44.7	0.5	66.8				
				SPZ	eLg	40	10.	1.1	39.0				No horizontals

CODE	Station	Distance Degrees	Distance km	Component	Phase	Obs. Arrival Time 1900 Hrs. Min.	Sec.	Period T Sec.	Maximum Amplitude A/T (mμ/sec)	Magnitude M_b	M_s	J. B. Residual	Remarks
ATL	Atlanta Georgia	18.99	2111	SPZ	eP	34	25.5	1.1	22.7	4.4	4.2	-0.1	
				SPZ	e(PP)	34	37.0	1.0	13.5				
				SPN	eLg	39	52.5	2.3	24.6				
				SPE	eLg	39	52.5	1.4	11.4				
				LPZ	LR	41	27.	12.0	64.0				
*PG-BC	Prince George British Columbia Canada	20.31	2259	SPZ	eP	34	39.6	0.6	38.5	4.7	4.6	-0.7	
				LPZ	LR	42	43.	13.0	69.2				
CLE	Cleveland Ohio	20.47	2278	SPE	eP	34	41.4	1.2	704.0			-0.7	No SPZ seismogram
				SPE	eLg	40	56.8	1.2	650.0				
				SPN	eLg	41	01.8	1.1	669.0				
				LPE	(LQ)	39		36.0	62.6				No LPZ seismogram
FSJ	Fort St. James Canada	21.29	2367	SPZ	eP	34	50.4	1.0	35.0	4.7	4.7	0.0	
BLA	Blacksburg Virginia	21.40	2378	SPZ	eP	34	50.9	1.0	65.0	5.4	4.9	-0.7	
				SPN	eLg	41	35	1.1	61.5				
				SPE	eLg	41	35.	0.9	52.9				
				LPN	LQ	41	22.	15.0	38.8				
				LPZ	LR	42	40.	11.0	193.0				
MRG	Morgantown West Virginia	21.60	2400	SPZ	eP	34	53.6	1.3	114.8	5.2	5.2	0.0	
				SPN	eLg	41	30.	1.9	307.0				
				SPE	eLg	41	44.	1.6	107.0				

CODE	Station	Distance Degrees	Distance km	Component	Phase	Obs. Arrival Time 1900 Hrs. Min.	Obs. Arrival Time 1900 Hrs. Sec.	Period T Sec.	Maximum Amplitude A/T (mμ/sec)	Magnitude M_B	Magnitude M_S	J.B. Residual	Remarks
SCP	State College Pennsylvania	23.20	2578	SPZ	eP	35	08.8	1.2	13.5	5.2	4.4	-0.7	
				SPN	eLg	42	24.	1.0	45.0				
				SPE	eLg	42	20.	0.9	38.0				
				LPN	LQ	42	30.	12.0	41.7				
				LPZ	LR	43	57.	10.0	33.3				
FCC	Fort Churchill Canada	23.71	2633	SPZ	eP	35	14.3	1.2	58.3	4.9	5.0	0.1	
				SPN	eLg	42	50.	1.4	11.8				
				SPE	eLg	43	08.	1.4	14.2				
WSC	Washington Science Center Maryland	23.82	2644	SPZ	eP	35	16.5	(1.5)	20.0	4.7	4.6	1.0	
OTT	Ottawa Canada	25.17	2800	SPZ	eP	35	28.5	1.0	78.4	5.4	5.3	0.1	
				SPN	eLg	43	32.	1.7	73.5				
				SPE	eLg	43	32.	1.8	41.6				
				LPN	LQ	43	20.	12.0	57.2				
				LPZ	LR	45	06.	9.0	107.0				
OGD	Ogdensburg New Jersey	25.66	2850	SPZ	eP	35	35.7	1.4	116.3	5.6	5.5	2.6	
				SPN	eLg	43	49.	1.5	22.6				
				SPE	eLg	43	56.	1.3	12.3				
				LPN	LQ	43	34.	14.0	15.3				
				LPZ	LR	45	19.	8.5	91.5				
YKC	Yellow Knife Canada	26.22	2911	SPZ	eP	35	36.6	0.6	10.4	5.5	4.5	-1.5	
				SPE	eLg	44	46.	1.8	7.42				No Lg on SPN

CODE	Station	Distance Degrees	km	Com-ponent	Phase	Obs. Arrival Time 1900 Hrs. Min.	Sec.	Period T Sec.	Maximum Amplitude A/T (mμ/sec)	Magnitude M_B	M_S	J.B. Residual	Remarks
PAL	Palisades New York	26.20	2911	SPZ	eP	35	37.3	1.3	16.7	4.8	4.7	-0.8	
				SPN	eLg	43	41.	1.4	51.4				
				SPE	eLg	44	04.	1.5	4.4				
				LPZ	LR	45	21.	18.0					No response curve
MNT	Montreal Canada	26.65	2962	SPZ	eP	35	41.3	1.1	30.4	5.0	5.0	-0.9	
				SPN	eLg	44	35.	1.2	37.6				
				SPE	eLg	44	50.	1.2	12.5				
				LPN	LQ	43	58.	12.0	26.8				
				LPZ	LR	45	55.	10.0	50.0				
WES	Weston Massachusetts	28.10	3122	SPE	eLg	45	10.	1.5	12.7				No SPZ-inoperative
				SPN	eLg	44	58.	1.3	37.1				
				LPN	LQ	44	30.	10.0	43.5				
				LPZ	LR	46	49.	10.0	71.7				
BLC	Baker Lake Canada	28.48	3167	SPZ	eP	35	57.1	1.0	7.2	4.5		-1.6	
				SPN	eLg	45	46.	1.2	9.5				
				SPE	eLg	45	53.	1.5	11.1				
SFA	Seven Falls Canada	29.78	3200	SPZ	eP	36	00.3	1.1	4.7	4.3		-1.3	
				SPN	eLg	45	25.	1.5	12.1				
				SPE	eLg	45	25.	1.3	4.1				
				LPN	LQ	45	12.	12.0	78.3				
				LPZ	LR	46	58.	12.0	83.5				

CODE	Station	Distance Degrees	Distance km	Com-ponent	Phase	Obs. Arrival Time 1900 Hrs. Min.	Obs. Arrival Time 1900 Hrs. Sec.	Period T Sec.	Maximum Amplitude A/T (mμ/sec)	Magnitude M_B	Magnitude M_E	J.B. Residual	Remarks
*WH2YK	White Horse Yukon Territory Canada	29.79	3314	SPZ	eP	36	(09.7)	0.7	4.1	4.2		-0.8	
*HN-ME	Houlton Maine	30.65	3406	LPT	LQ	46	15.	15.0	33.6				
				LPZ	LR	47	09.	13.0	45.9				
CMC	Coppermine Canada	31.52	3500	SPZ	eP	36	24.6	1.0	4.0	4.3		-1.0	
				SPZ	e(PP)	37	33.8	1.4	7.2				
				SPZ	ePcP	39	15.5	1.2	2.4				
				SPN	eLg	47	40.	1.3	22.0				
				SPE	eLg	47	26.	1.7	11.8				
*SV3QB	Schefferville Quebec, Canada	32.96	3665	SPZ	eP	36	36.0	0.7	9.9	4.7		-2.3	
				LPR	LQ	47	14.	20.0	6.0				
				LPZ	LR	49	34.	12.0	56.3				
SCH	Schefferville Canada	32.94	3662	SPZ	eP	36	37.0	1.2	18.1	5.0		-1.3	
				SPN	eLg	47	40.	1.0	10.0				
				SPE	eLg	47	40.	1.0	8.4				
FBC	Frobisher Bay Canada	35.75	3973	SPZ	eP	37	01.2	0.6	3.7	4.2		-1.0	
				SPN	eLg	48	55.	1.2	6.0				
				SPE	eLg	48	51.	1.2	4.8				
				LPZ	LR	50	06.	9.5	69.3				

CODE	Station	Distance Degrees	Distance km	Component	Phase	Obs. Arrival Time 1900 Hrs. Min.	Sec.	Period T Sec.	Maximum Amplitude A/T (mμ/sec)	Magnitude M_b	M_s	J.B. Residual	Remarks
BLR	Black Rapids Alaska	35.59	3956	SPZ	eP	37	01.5	0.5	916.0	6.6		0.5	
GIL	Gilmore Creek Alaska	36.96	4100	SPZ	eP	37	13.0					0.6	Telegraphic report
PJD	Pedro Dome Alaska	35.99	4111	SPZ	eP	37	13.3	0.6	526.0	6.2		0.3	
COL	College Alaska	37.03	4111	SPZ	iPc	37	13.6	0.7	66.9	5.4		0.6	
				SPZ	e(PcP)	39	17.0	2.5	70.0				
BIG	Big Mountain Alaska	38.17	4244	SPZ	e(P)	37	22.7	0.4	196.5	5.8		0.0	
RES	Resolute Bay Canada	38.55	4285	SPZ	eP	37	24.0	1.1	4.8	4.1		-1.7	
				SPN	eLg	46		1.1	12.8				
				SPE	eLg	46		1.6	14.2				
				LPZ	LR	53	10.	9.0	51.0				
TNN	Tanana Alaska	38.74	4306	SPZ	eP	37	28.1	0.5	200.0	5.7		0.7	

CODE	Station	Distance Degrees	Distance km	Com-ponent	Phase	Obs. Arrival Time 1900 Hrs. Min.	Obs. Arrival Time 1900 Hrs. Sec.	Period T Sec.	Maximum Amplitude A/T (mμ/sec)	Magnitude M_B	Magnitude M_S	J.B. Residual	Remarks
**SVW	Sparrevohn Alaska	38.83	4311	SPZ	eP	37	28.3	0.5	642.0	6.2		0.1	
*NP-NT	Mould Bay Northwest Territories Canada	40.06	4453	SPZ SPZ	eP ePcP	37 39	37.9 42.	0.7 0.6	35.7 3.8	5.0		-0.1	
MBC	Mould Bay Canada	40.03	4444	SPZ	iPc	37	38.3	1.0	18.2	4.7		0.3	
BRW	Barrow Alaska	43.01	4478	SPZ	eP	38	02.6	(0.9)	50.0	5.2		0.1	
ADK	Adak Alaska	50.04	5565	SPZ	eP	38	(50.4)	(0.6)	94.0	4.7		-1.9	
NOR	Nord Greenland	54.04	6006	SPZ	e(P)	39	27.5					-0.4	Marginal data
KTG	Kap Tobin Greenland	54.38	6044	SPZ	e(P)	39	28.2	1.0	16.0	5.0		-2.3	
NNA	Nana Peru	56.22	6244	SPZ	e(P)	39	44.6					0.1	Marginal data

**Station code in Figure 1 shown as SV/

CODE	Station	Distance Degrees	Distance km	Com-ponent	Phase	Obs. Arrival Time 1900 Hrs. Min.	Obs. Arrival Time 1900 Hrs. Sec.	Period T Sec.	Maximum Amplitude A/T (mμ/sec)	Magnitude M_B	Magnitude M_E	J.B. Residual	Remarks
ARE	Arequipa Peru	62.69	6967	SPZ	eP	40	27.5	(1.2)	(22.1)	5.3		-2.0	
KEV	Kevo Finland	68.75	7644	SPZ	e(P)	41	04.8					-2.6	Marginal data
KIR	Kiruna Sweden	68.65	7633	SPZ	e(P)	41	05.1	(0.5)	(45.2)	5.7		-1.7	
FLN	Foliniere France	72.97	8111	SPZ	e(P)	41	32.6	1.5	21.2	5.2		-0.6	
GRR	Gorron France	73.00	8111	SPZ	e(P)	41	33.1	0.9	15.2	5.1		-0.3	
SSC	St. Sauveur De Carouge France	73.28	8144	SPZ	e(P)	41	34.6	0.8	7.6	4.8		-0.4	
UPP	Uppsala Sweden	73.64	8178	SPZ	e(P)	41	35.5	1.3	47.9	5.6		-1.3	
NUR	Nurmijarvi Finland	75.44	8378	SPZ	e(P)	41	45.5	0.7	11.0	5.0		-1.8	
SSF	Saint Saulges France	76.10	8456	SPZ	e(P)	41	50.1	1.4	28.3	5.4		-1.2	

CODE	Station	Distance Degrees	Distance km	Component	Phase	Obs. Arrival Time 1900 Hrs. Min.	Obs. Arrival Time 1900 Hrs. Sec.	Period T Sec.	Maximum Amplitude A/T (mμ/sec)	Magnitude M_b	Magnitude M_s	J.B. Residual	Remarks
LOR	Lormes France	76.19	8467	SPZ	e(P)	41	50.5	1.1	29.6	5.4		-1.3	
HLE	Halle Germany	77.33	8589	SPZ	e(P)	41	56.3	(1.0)	(19.6)	5.2		-1.7	
*CLL	Collmberg Germany	77.93	8656	SPZ	e(P)	42	00.0					-1.3	Telegraphic report
SOP	Sopron Hungary	82.16	9133	SPZ	eP	42	24.0	(1.5)	14.9	5.1		0.0	
PSZ	Piszkesteto Hungary	83.46	9278	SPZ	eP	42	31.6	(1.5)	(15.8)	5.2		0.8	
MTJ	Mount Tsukuba Japan	84.31	9367	SPZ	e(P)	42	33.2	(0.7)	1.9	4.3		-2.1	
MAT	Matsushiro Japan	85.23	9467	SPZ	eP	42	39.3	1.0	39.0	5.6		-0.6	

World Wide Standard Seismograph Stations underlined;temporary stations detonated by IR and R

*LRSM stations from "GASBUGGY Report"

For station coordinates see Coast and Geodetic "Seismograph Station Abbreviations" book.

e = emergent; i = impulsive; c = compression; ( ) = doubtful values or phases

TABLE 3 -- SURFACE WAVE MAGNITUDE COMPUTATIONS

$M_S = \log_{10}(A/T) + 1.66 \log_{10} \Delta^\circ + 3.3$

Station	Δ°	LPZ A mm	LPZ T sec	LPZ A/T mμ/sec	LPN A mm	LPN T sec	LPN A/T mμ/sec	LPE A mm	LPE T sec	LPE A/T mμ/sec	M_B	M_R	LPZ M_S	LPN M_S	LPE M_S	
GOL	3.35	5.6	8.0	389.0	4.0	6.0	555.5	2.0	(4.0)	500.0	5.7	4.8	3.76	3.91	3.87	A - Amplitude in mm (C-P)
* UBO	4.08		16.0	485.4							5.8	5.1	4.00			T - Period (sec)
* LC-	4.30		13.0	136.8							5.3	4.8	3.49			A/T - microns (μ)
* KN-	4.52		13.0	256.7							6.2	5.1	3.79			Δ - distance in degrees
TUC	5.26	4.5	8.0	313.0	3.88	5.0	646.6	3.61	5.0	600.8	5.0	4.4	4.00	4.31	4.28	
DUG	5.63	17.0	10.0	315.0	7.67	(8.0)	252.0	12.2	10.0	225.0	5.2	5.0	4.05	3.95	3.90	
* CQ-	5.92		14.0	208.5							4.9	4.5	3.90			
* PQ-	6.55		15.0	158.4							5.4	4.8	3.85			
* TL-	6.87		16.3	57.9							5.9	4.4	3.45			
* WMO	7.28		12.0	350.1							5.3	4.6	4.28			
RCD	7.99	1.2	8.0	83.6							5.5	4.1	3.72			Horizontal components noisy
THP	8.09	3.2	11.0		2.7	7.0		4.5	4.2		5.6	4.2				No LP response curve
* WZ-	8.49		12.0	226.7							5.0	4.3	4.20			
* WN-	8.49		12.0	151.4							6.3	4.9	4.02			
* HL2	8.82		13.0	227.9							5.3	4.6	4.23			
* MN-	8.86		13.0	242.0							4.9	4.3	4.26			
* BS-	9.13		15.0	79.0							5.8	4.3	3.79			
* LAO	10.03		16.0	32.7							6.0	4.5	3.50			
RBN	10.37	6.2	11.0	256.0				3.5	12.0	139.0			4.40		4.05	
* LN-	10.62		15.0	58.4							5.7	4.3	3.77			
* HV-	11.89		15.0	60.1							5.6	4.4	3.86			
* PH-	12.35		15.0	123.1							5.5	4.3	4.20			
SLM	13.59	6.2	8.0					6.3	5.6		6.3	5.6				No LP response curve
NEW	13.68	3.5	12.0	32.4	1.66	12.0	14.1	1.38	10.0	14.1	5.2	4.6	3.72	4.34	4.34	
SES	13.99	3.8	12.0	3.52							4.1	3.6	2.75			Horizontal components noisy
OXF	14.65	2.0	10.0	43.5	1.67	7.0	140.7	1.67	6.0	173.8	5.8	4.7	3.87	4.38	4.47	
* CC-	15.09		16.0	42.2							3.9	3.8	3.88			
PNT	15.53	7.6	10.5	144.0	5.2	10.5	95.2	3.4	11.0	59.5	5.3	4.8	4.34	4.26	4.05	
* LY-	16.23		17.0	83.5							4.7	4.4	4.23			
BLO	16.51	5.5	9.0		1.2	8.0		3.1	8.0		4.7	5.1				No LP response curve
* RK-	17.16		15.0	29.3							3.9	4.3	3.82			

Station	Δ°	LPZ A mm	LPZ T sec	LPZ A/T mμ/sec	LPN A mm	LPN T sec	LPN A/T mμ/sec	LPE A mm	LPE T sec	LPE A/T mμ/sec	MAGNITUDES M_B	M_E	LPZ M_S	LPN M_S	LPE M_S	
* CPO	17.51		17.0	173.4							4.2	4.4	4.60			
FFC	18.40				2.7	12.0	80.2				4.2	5.1		3.65		Vertical component noisy
ATL	18.99	2.0	12.0	64.0	0.6	13.0	17.7	1.5	11.5	50.1	4.4	4.2	4.23	3.67	4.12	
PG-	20.31		13.0	69.2							4.7	4.6	4.31			
CLE	20.50							3.0	18.0	463.8					5.15	No vertical component
BLA	21.40	10.2	11.0	193.0				2.5	10.0	52.1	5.4	4.9	4.80		4.23	
SCP	23.20	2.8	10.0	33.3				2.0	11.0	75.7	5.2	4.4	4.09		4.45	
OTT	25.17	2.9	9.0	107.0				1.7	9.5	59.5	5.4	5.3	4.65		4.39	
OGD	25.66	1.4	8.5	91.5				0.7	10.0	31.8	5.6	5.5	4.60		4.14	
MNT	26.65	1.4	10.0	50.0				1.4	7.0	100.0	5.0	5.0	4.37		4.67	
WES	28.10	3.3	10.0	71.7				2.2	11.0	41.6			4.56		4.32	
SFA	28.78	1.6	12.0	83.5				1.2	12.0	62.5	4.3		4.64		4.52	
* HN-	30.65		13.0	45.9									4.42			
* SV3-	32.96		12.0	56.3							4.7		4.57			
FBC	35.75	2.5	9.5	69.3	0.6	12.0	12.5	1.5	10.0	37.5	4.2		4.72	3.98	4.45	
RES	38.55	1.1	9.0	51.0							4.1		4.64			

World Wide Standard Seismograph Stations Underlined
* LRSM Stations

TABLE 4 -- Hypocenter Determinations

Number of Stations	Depth km	Origin Time	Coordinates Lat.°	Long.°	Shift (km) from Actual Location Lat.	Long.	Shift Direction	Remarks
153	0*	19-30-00.1*	36.678*	107.208*	---	---	---	J.B. Tables
147	0*	19-29-59.3	36.688	107.174	1.11	3.07	ENE	J.B. Tables
145	3	19-29-59.8	36.680	107.184	0.22	2.17	ENE	J.B. Tables
146	0*	19-30-01.8	36.636	107.165	4.66	3.85	SSE	Herrin Table (1968)

*Data intentionally restrained
Equivalent shift in kilometers per degree: Lat. 110.028; Long. 1.152

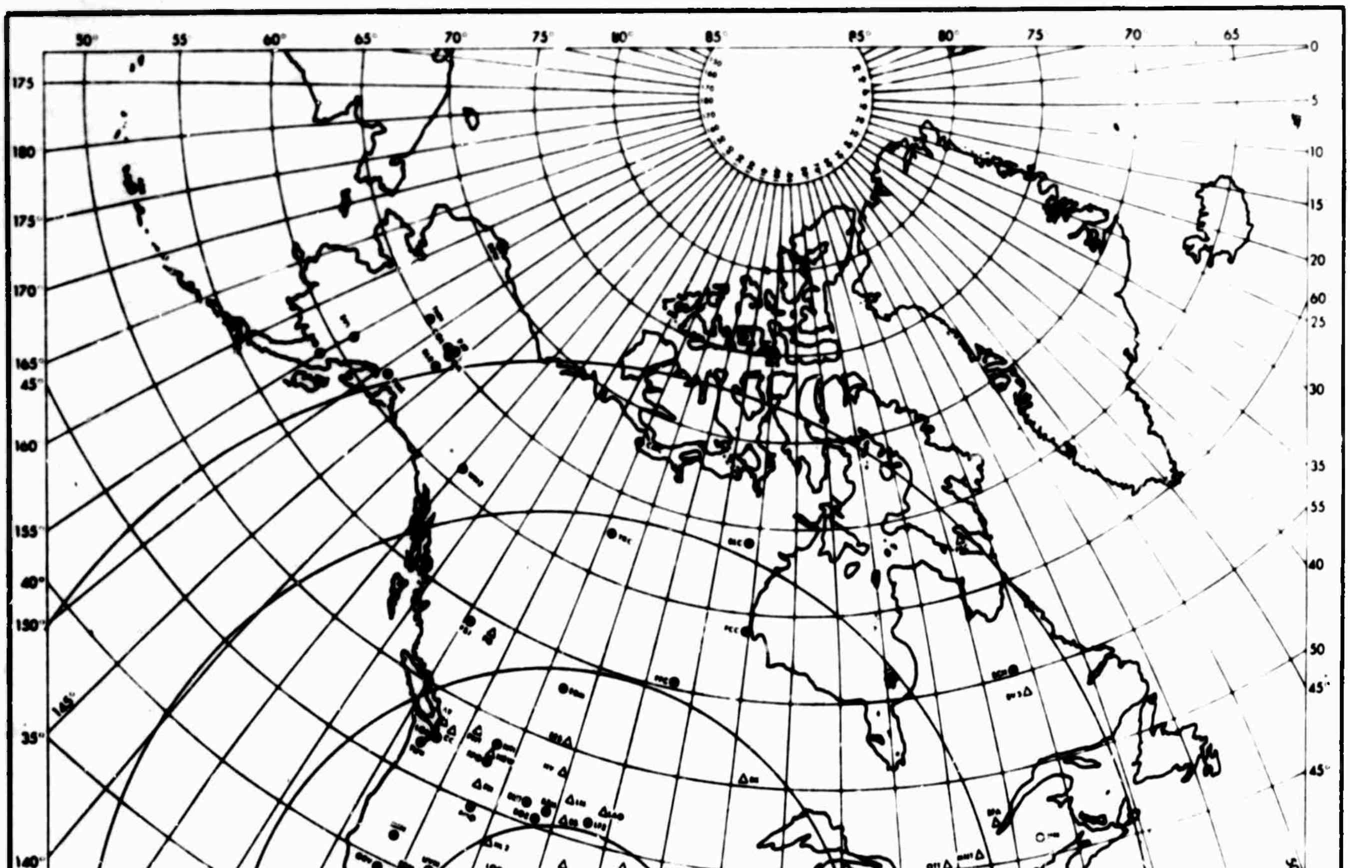

FIG. 1 SEISMOGRAPHIC STATIONS IN THE UNITED STATES, CANADA, ALASKA RECORDING SIGNALS FROM GASBUGGY EVENT. STATIONS ARE IDENTIFIED BY CODES GIVEN IN TABLE 1

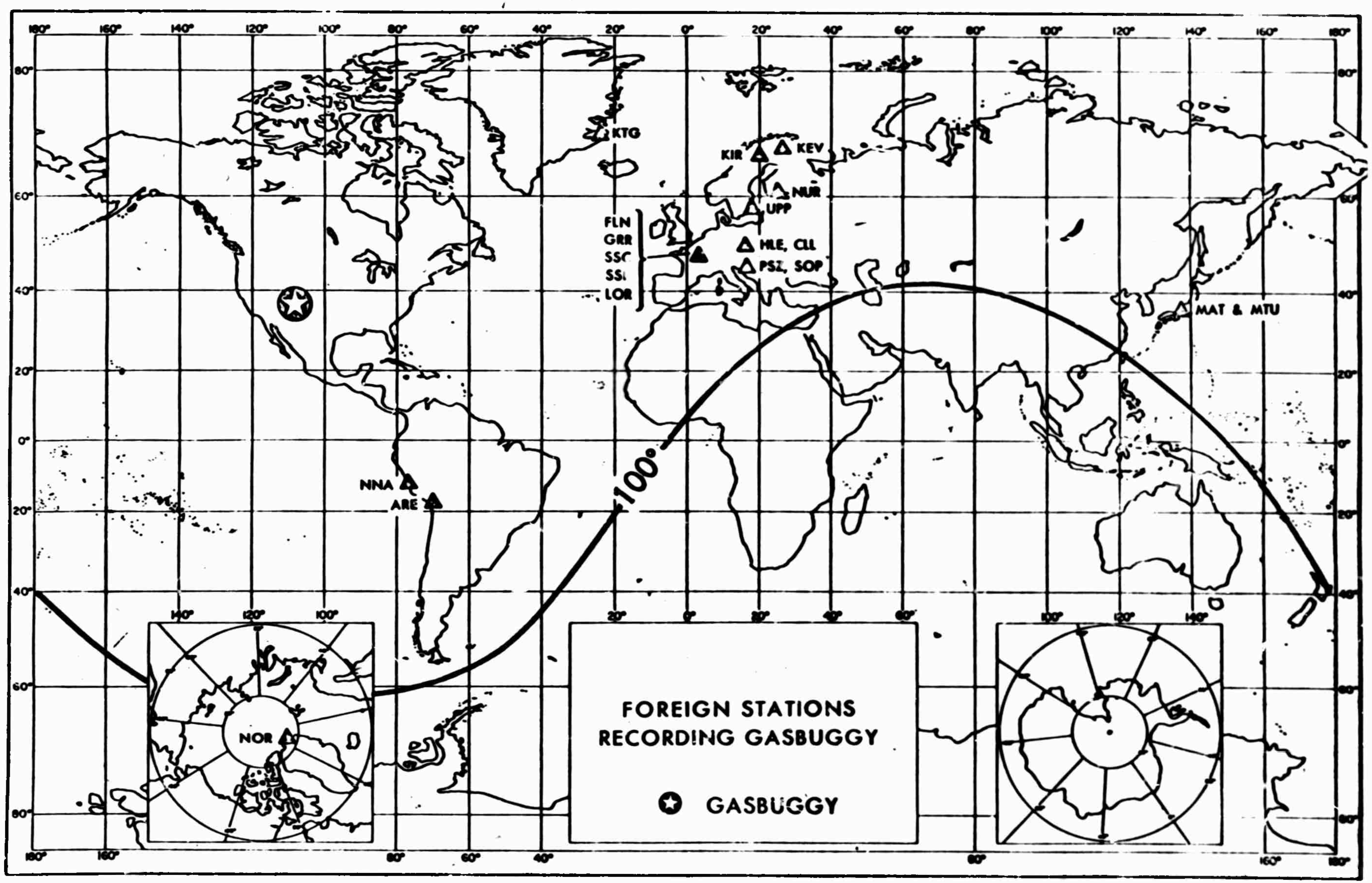

FIG. 2 DISTANT SEISMOGRAPHIC STATIONS RECORDING SIGNALS FROM GASBUGGY. THE SMOOTH CURVE IS AT A DISTANCE OF 100° FROM GASBUGGY SITE.

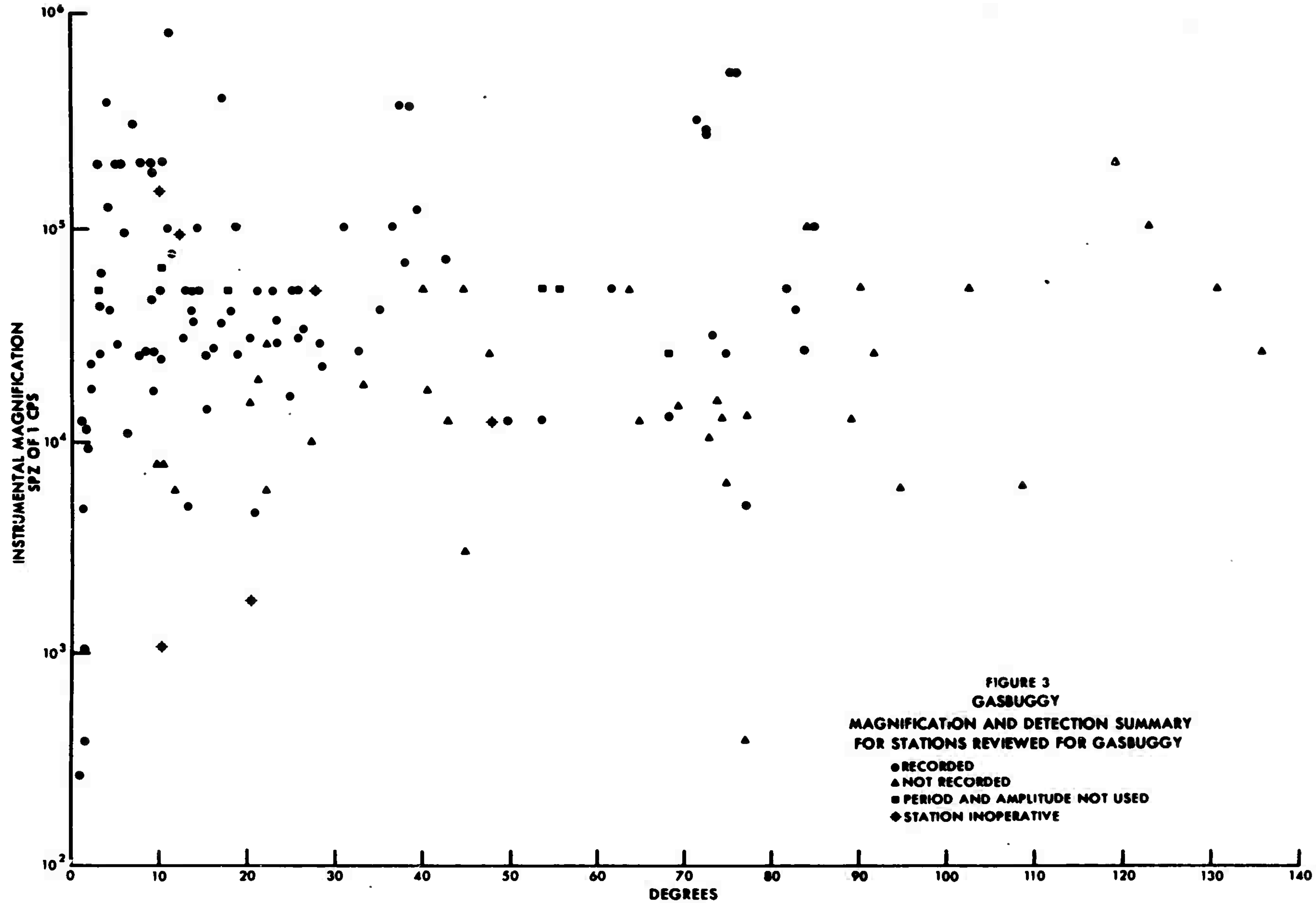

FIGURE 3
GASBUGGY
MAGNIFICATION AND DETECTION SUMMARY
FOR STATIONS REVIEWED FOR GASBUGGY

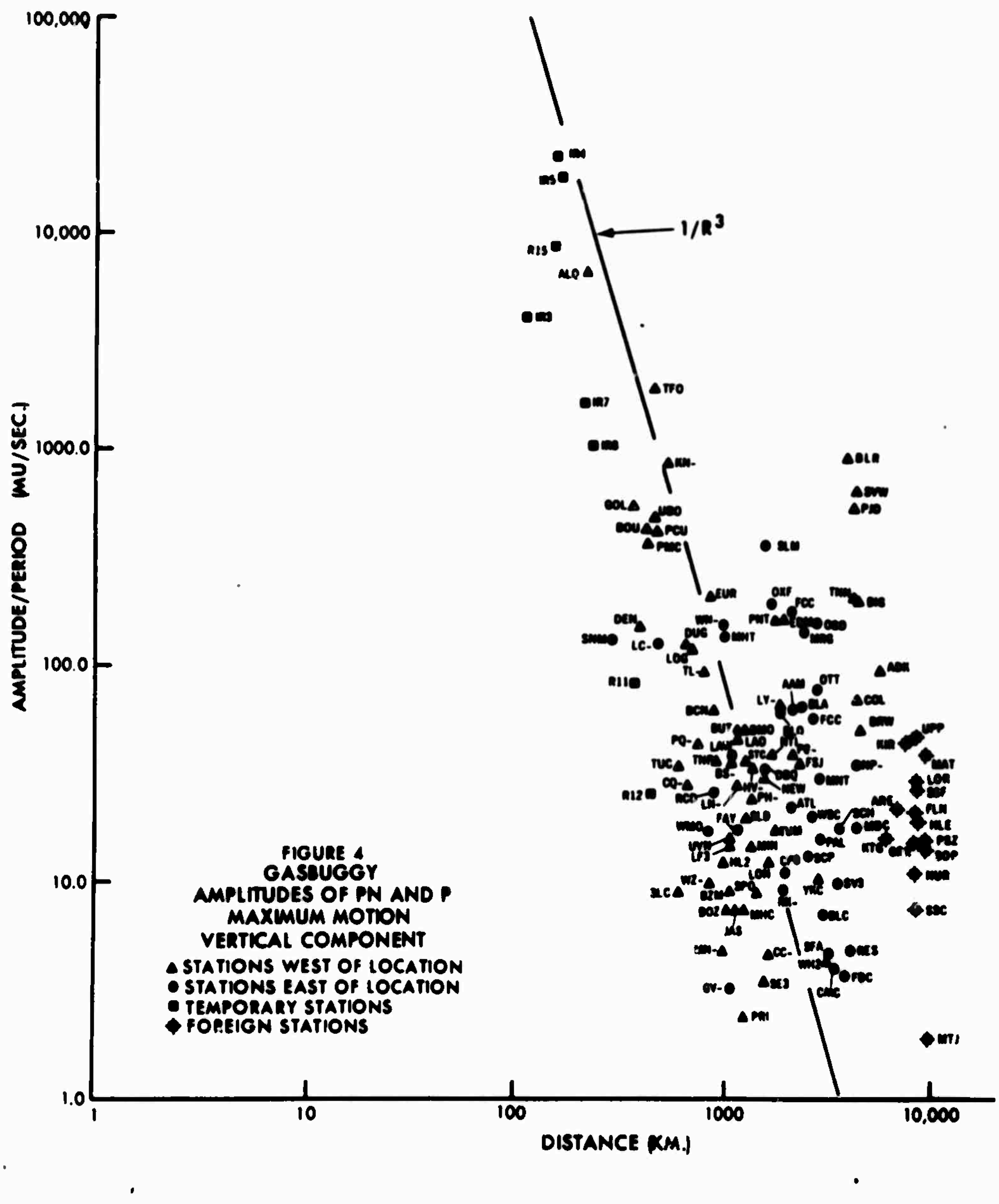

FIGURE 4
GASBUGGY
AMPLITUDES OF PN AND P
MAXIMUM MOTION
VERTICAL COMPONENT

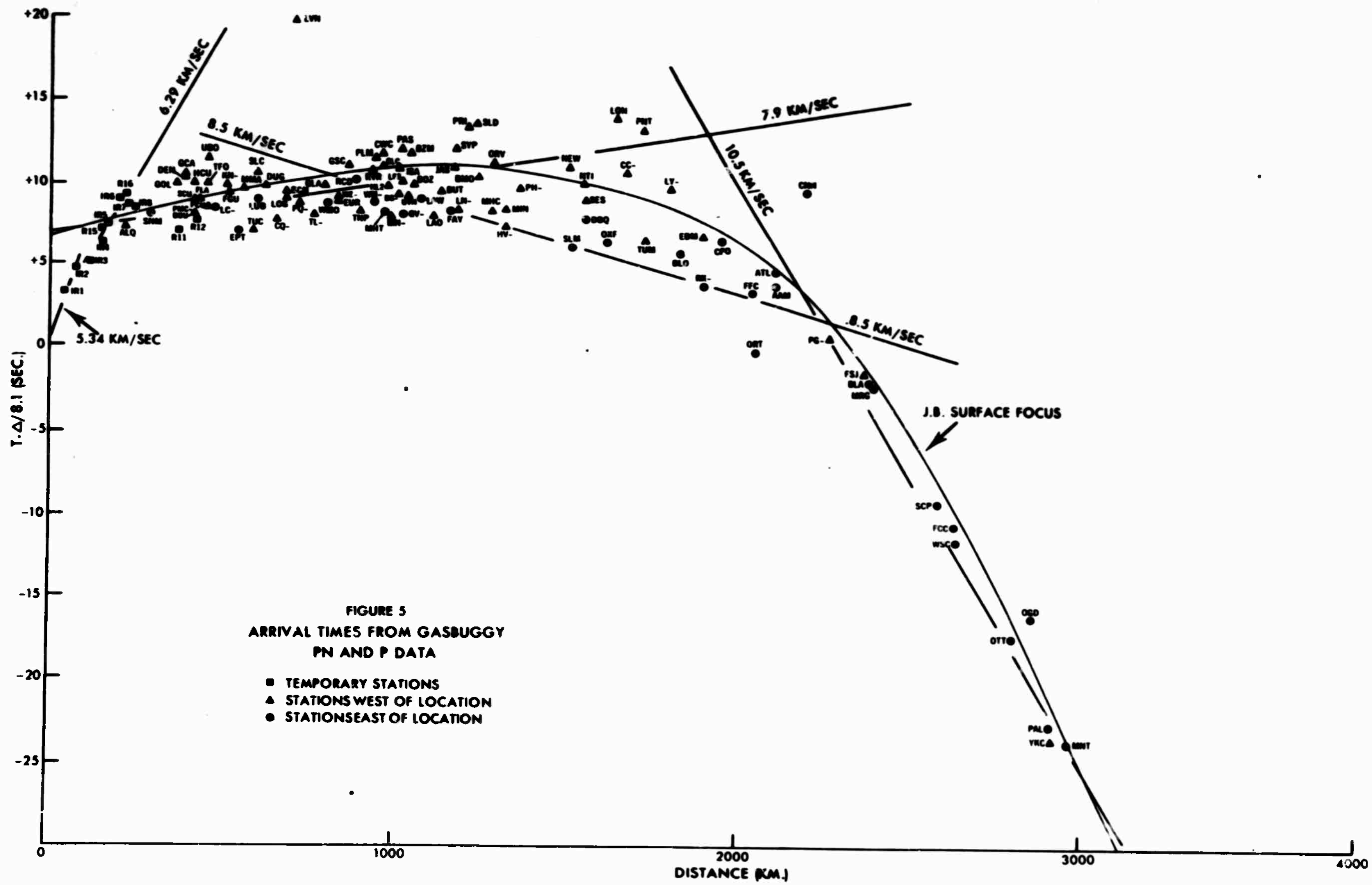

FIGURE 5
ARRIVAL TIMES FROM GASBUGGY
PN AND P DATA

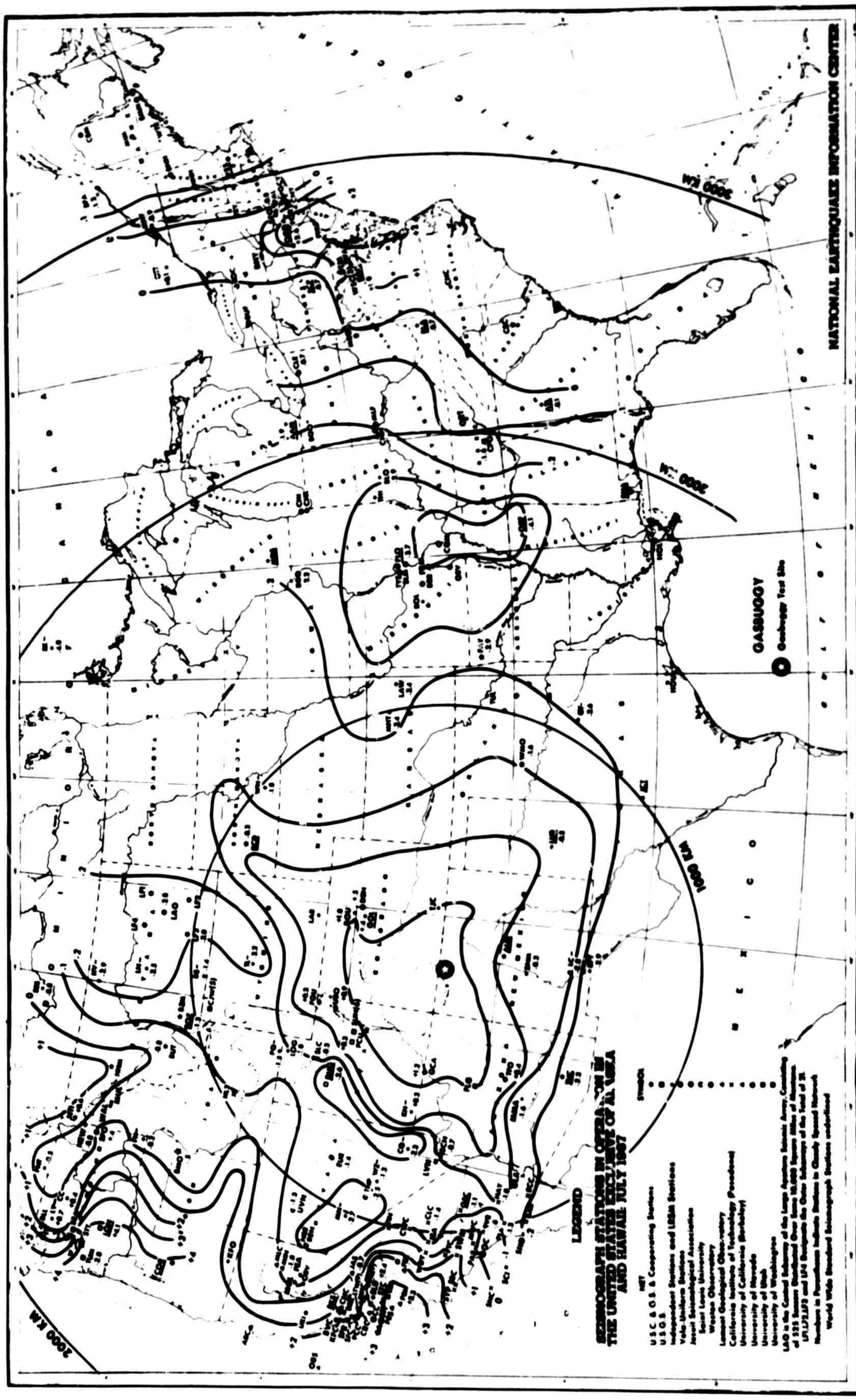

FIGURE 6 CONTOUR MAP OF P TRAVEL TIME RESIDUALS RELATIVE TO J.B. TABLES FOR SURFACE FOCUS.

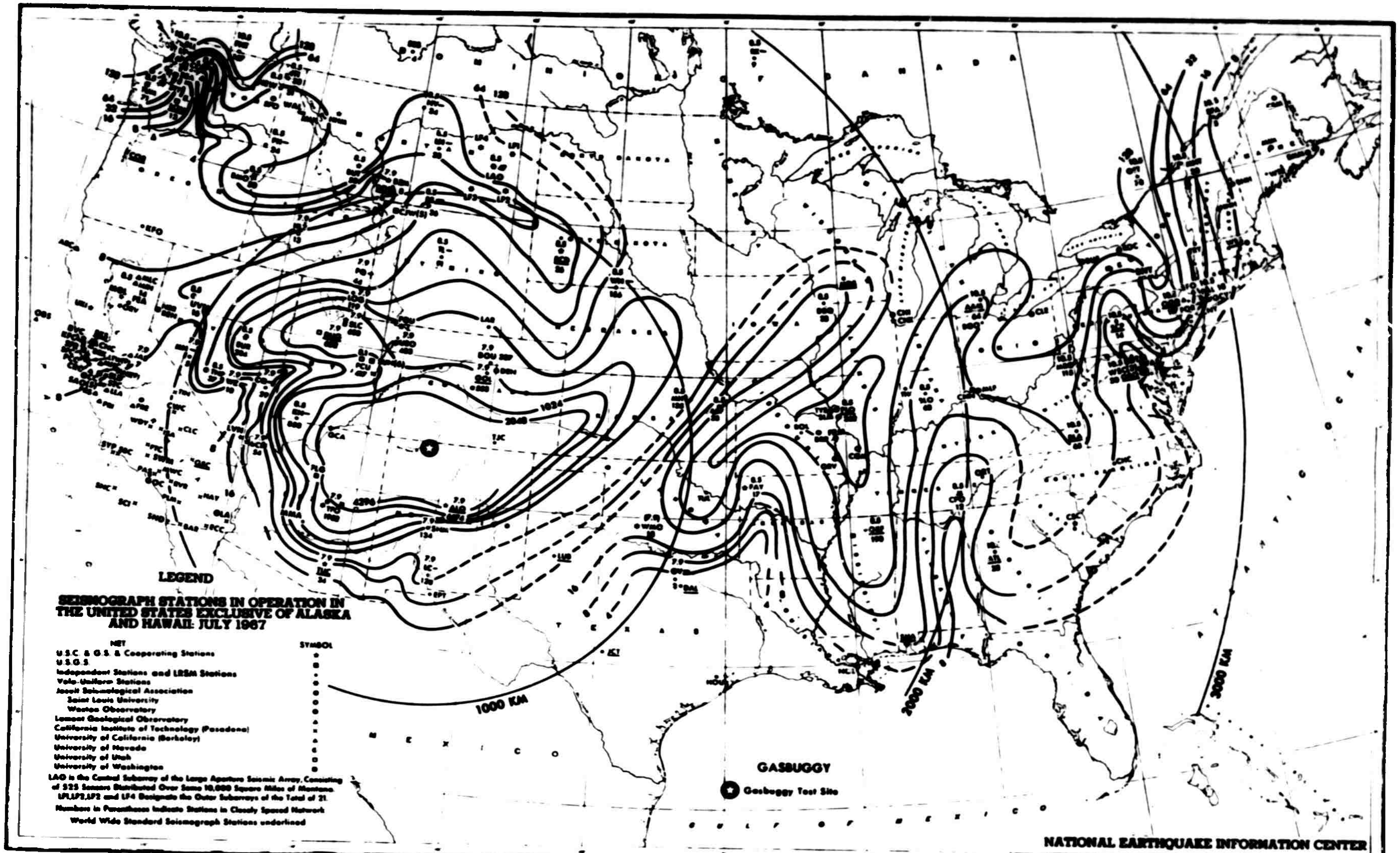

FIGURE 7 PATTERNS OF MAXIMUM AMPLITUDES OF PN AND P WAVES.
NUMBERS ABOVE STATION CODE REPRESENT APPARENT VELOCITIES
NUMBERS BELOW REPRESENT A/T AMPLITUDES (MU/SEC).

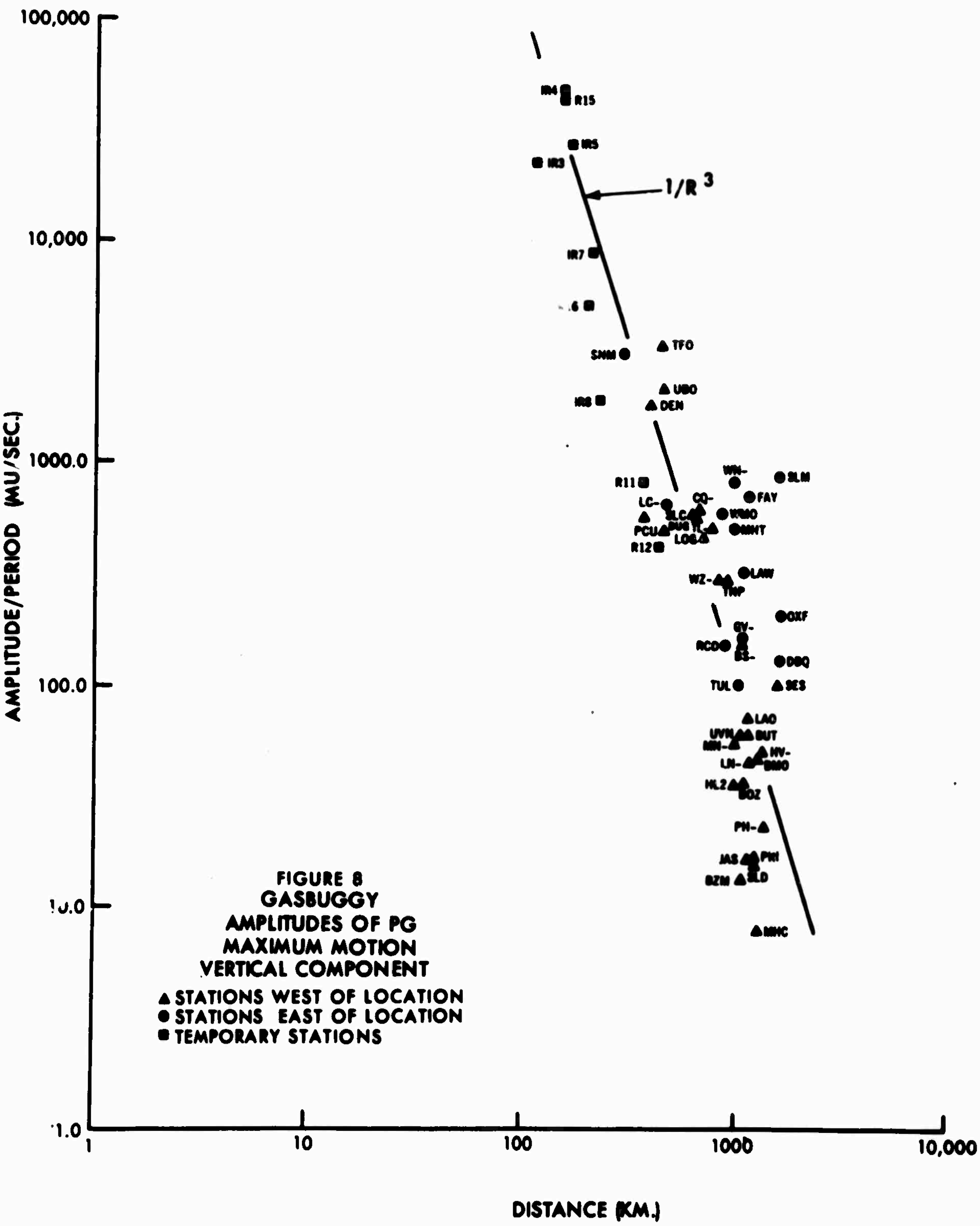

FIGURE 8
GASBUGGY
AMPLITUDES OF PG
MAXIMUM MOTION
VERTICAL COMPONENT

▲ STATIONS WEST OF LOCATION
● STATIONS EAST OF LOCATION
■ TEMPORARY STATIONS

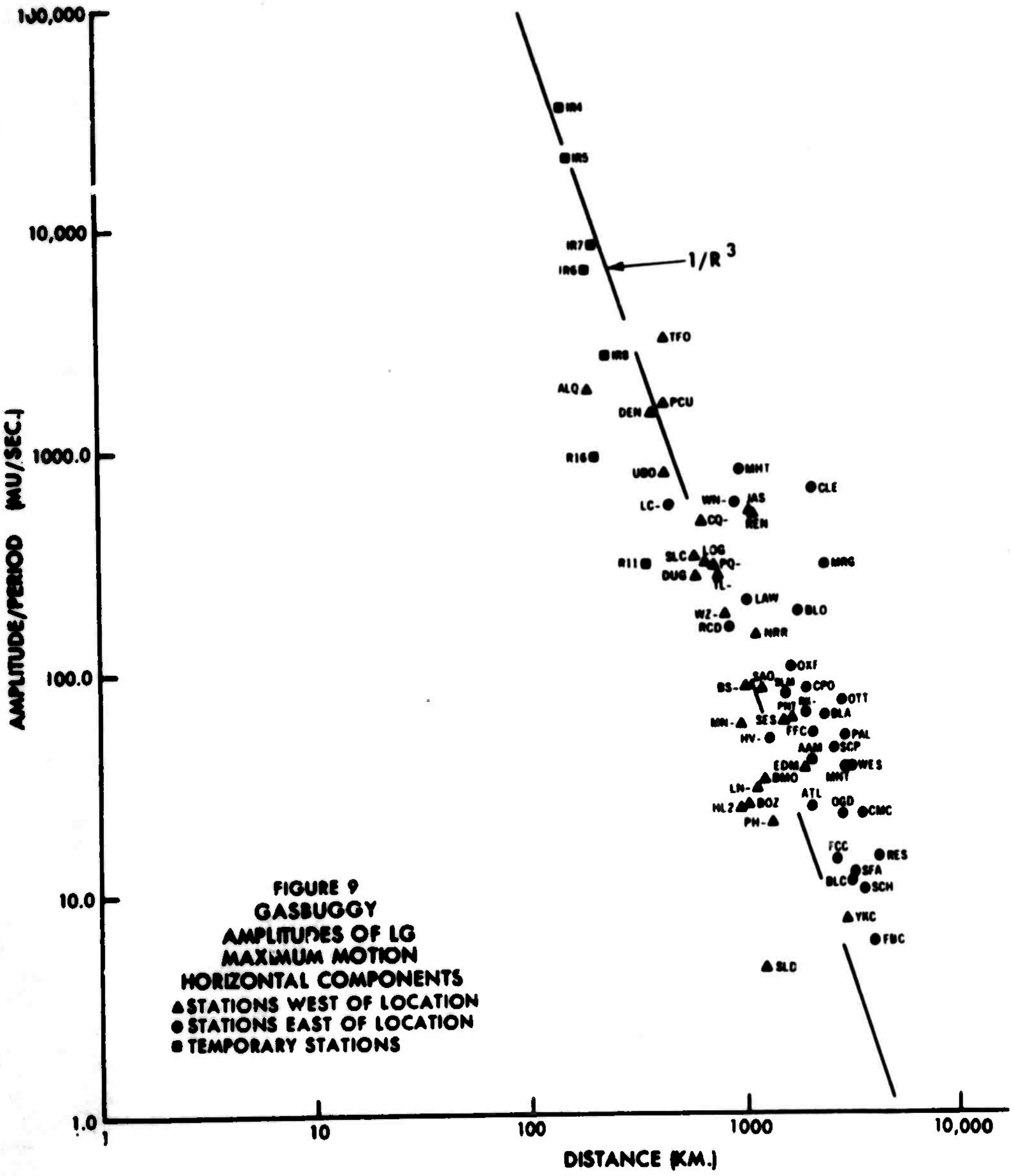
AMPLITUDE/PERIOD (MU/SEC.)
DISTANCE (KM.)
1/R 3
FIGURE 9
GASBUGGY
AMPLITUDES OF LG
MAXIMUM MOTION
HORIZONTAL COMPONENTS
▲ STATIONS WEST OF LOCATION
● STATIONS EAST OF LOCATION
■ TEMPORARY STATIONS

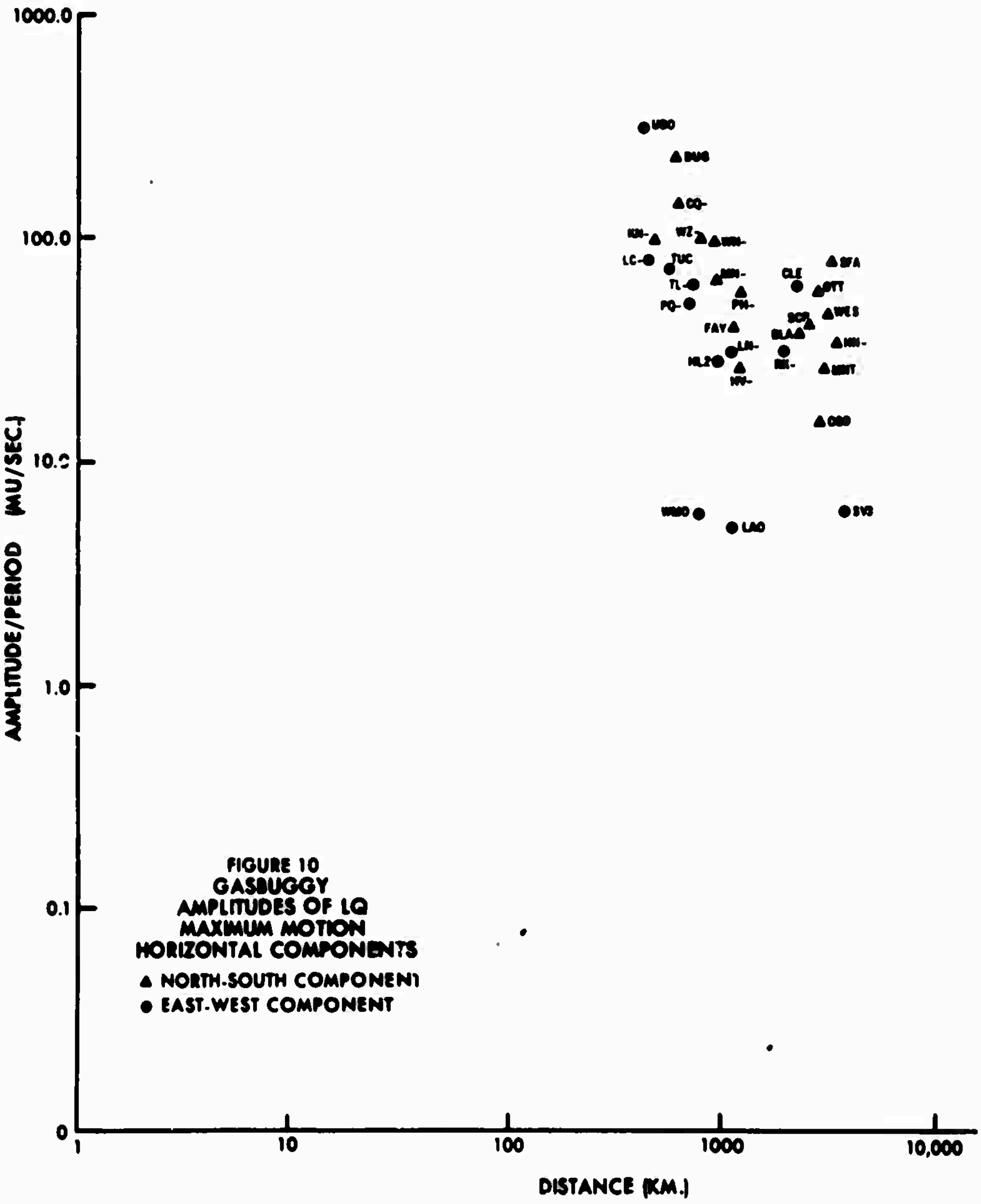

FIGURE 10
GASBUGGY
AMPLITUDES OF LQ
MAXIMUM MOTION
HORIZONTAL COMPONENTS

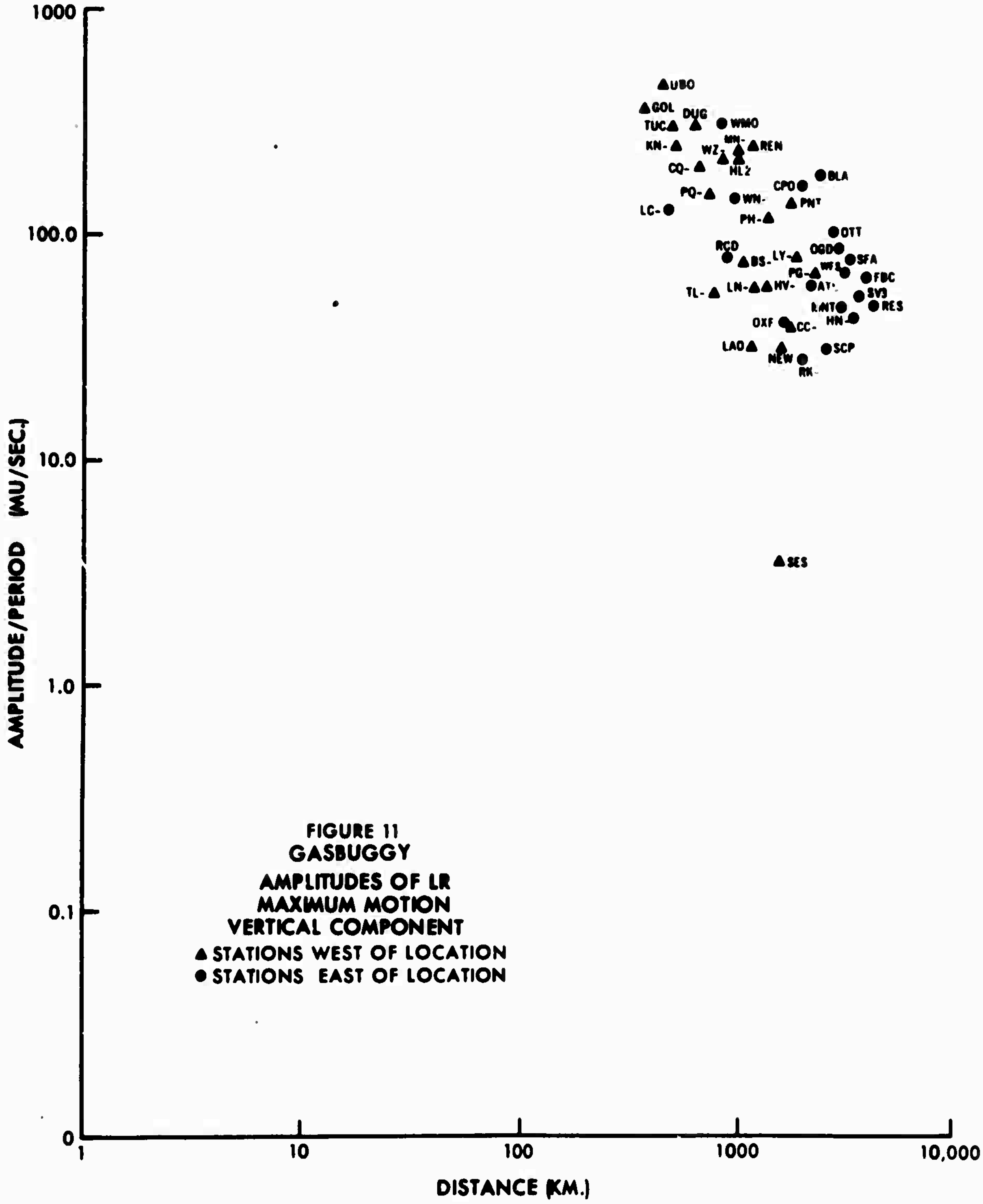

FIGURE 11
GASBUGGY
AMPLITUDES OF LR
MAXIMUM MOTION
VERTICAL COMPONENT
▲ STATIONS WEST OF LOCATION
● STATIONS EAST OF LOCATION

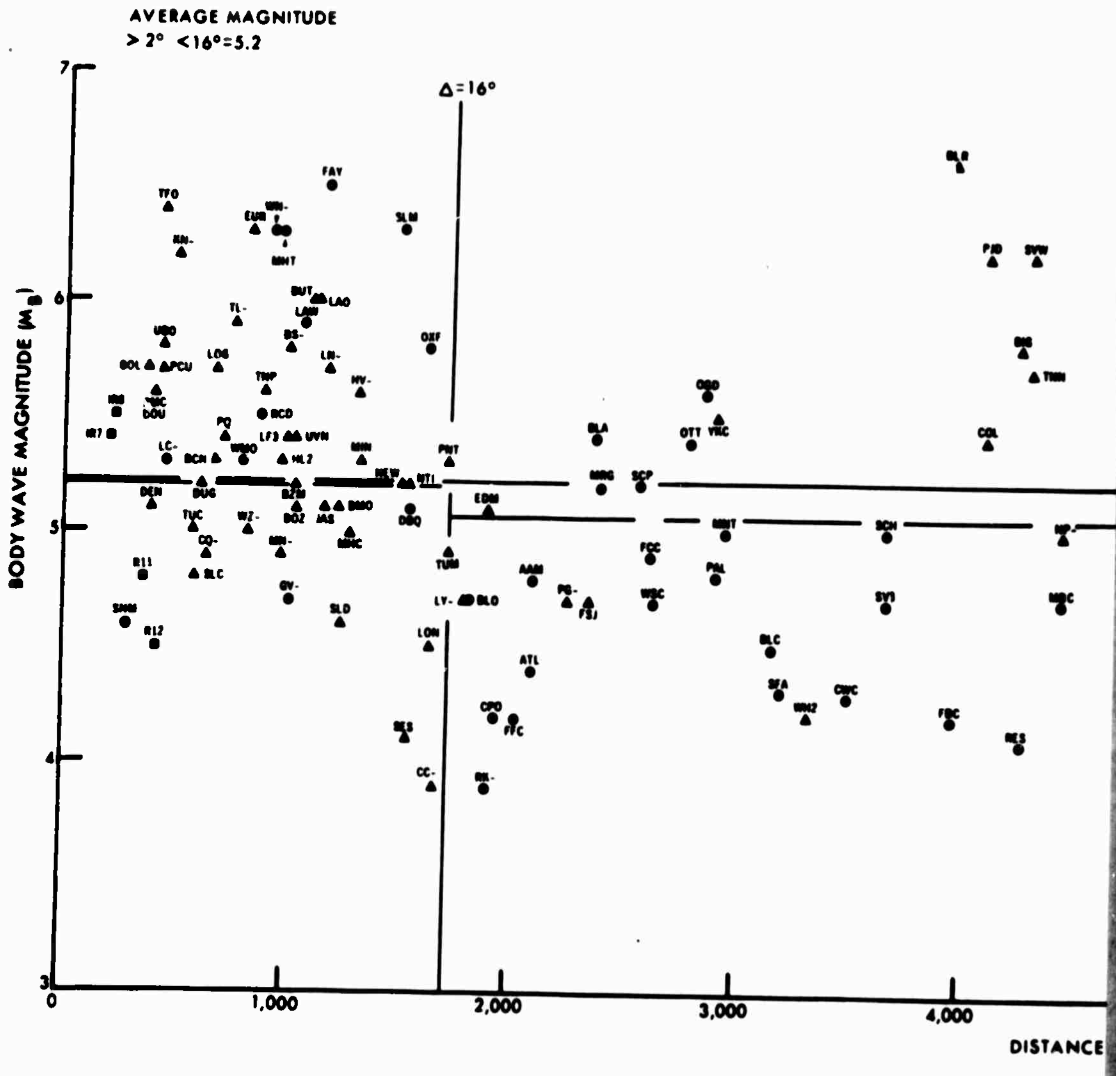

AVERAGE MAGNITUDE
> 2° < 16° = 5.2
Δ=16°
BODY WAVE MAGNITUDE (M_B)
DISTANCE
0
1,000
2,000
3,000
4,000
3
4
5
6
7

A

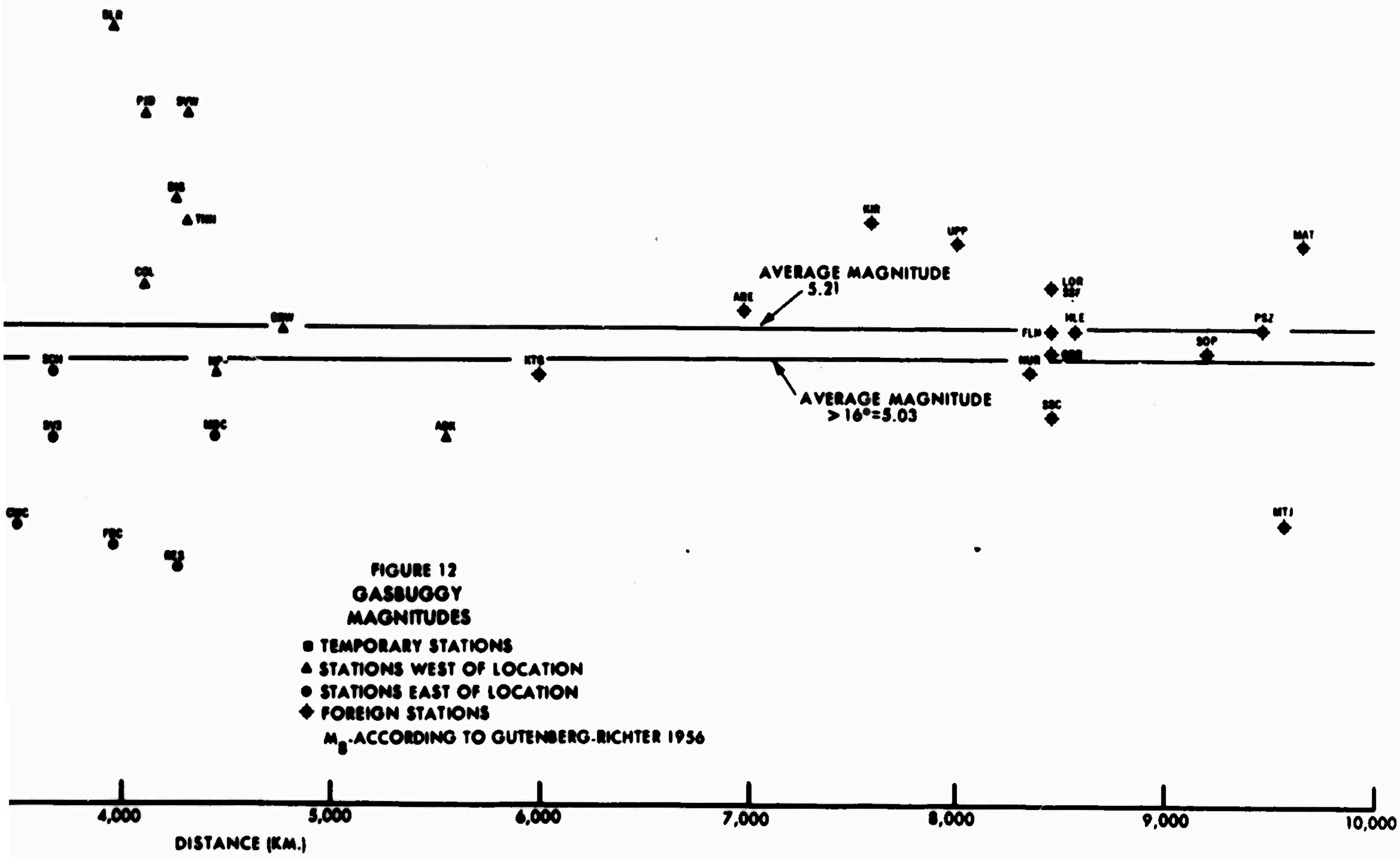

FIGURE 12
GASBUGGY
MAGNITUDES

P

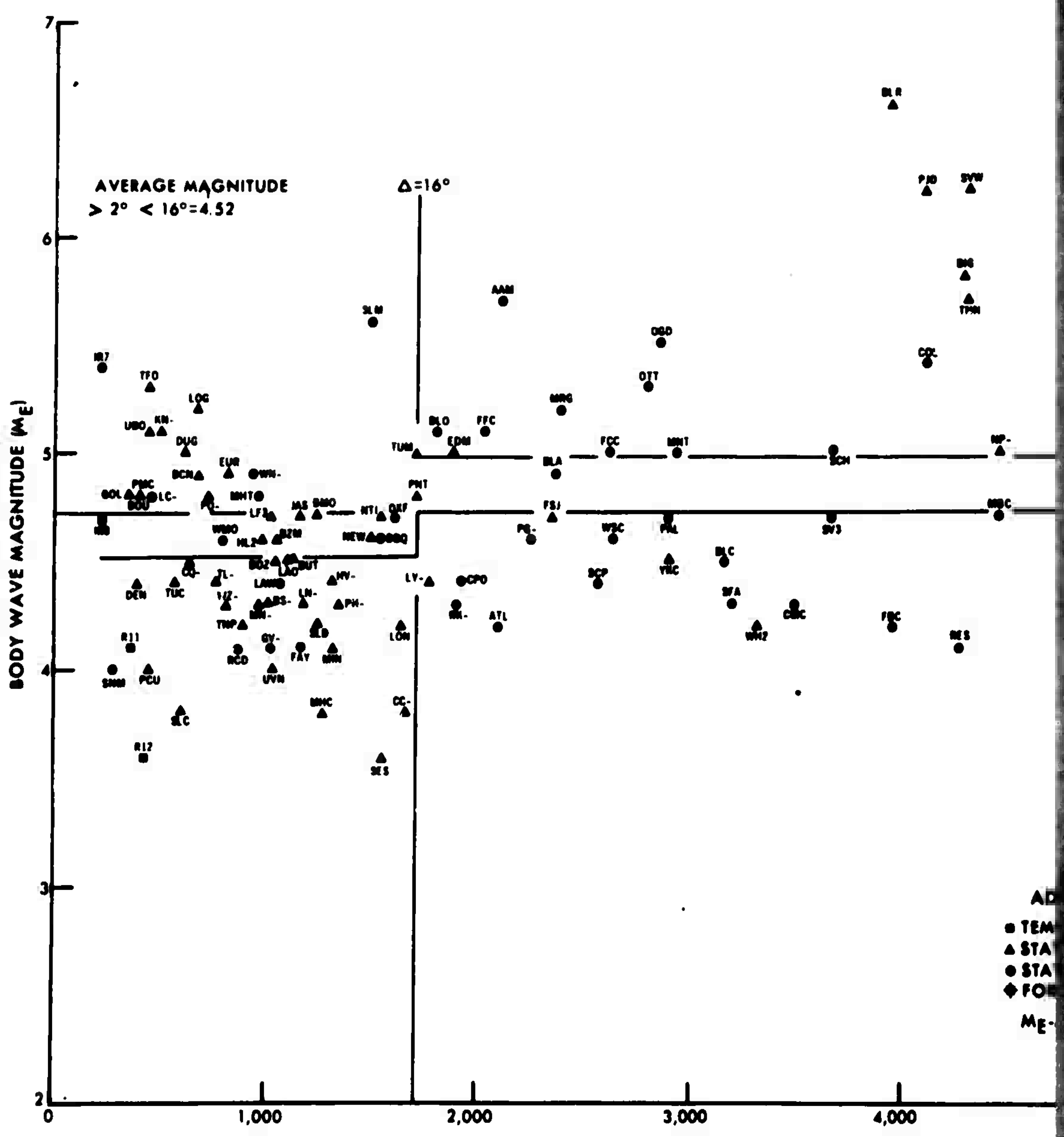
AVERAGE MAGNITUDE
> 2° < 16°=4.52
Δ=16°
BODY WAVE MAGNITUDE (M_E)
7
6
5
4
3
2
0
1,000
2,000
3,000
4,000

A

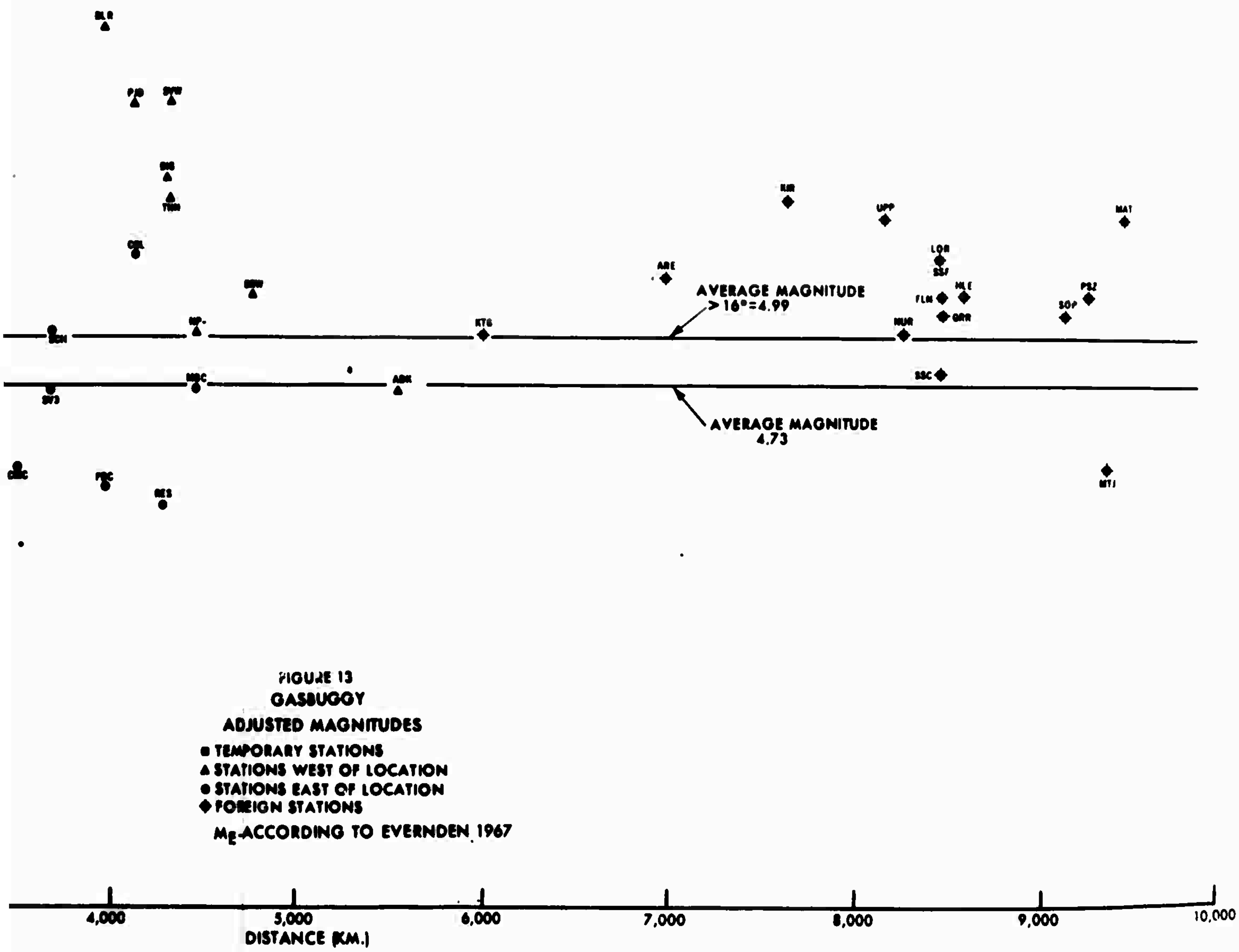

FIGURE 13
GASBUGGY
ADJUSTED MAGNITUDES
■ TEMPORARY STATIONS
▲ STATIONS WEST OF LOCATION
● STATIONS EAST OF LOCATION
◆ FOREIGN STATIONS
M_E ACCORDING TO EVERNDEN 1967

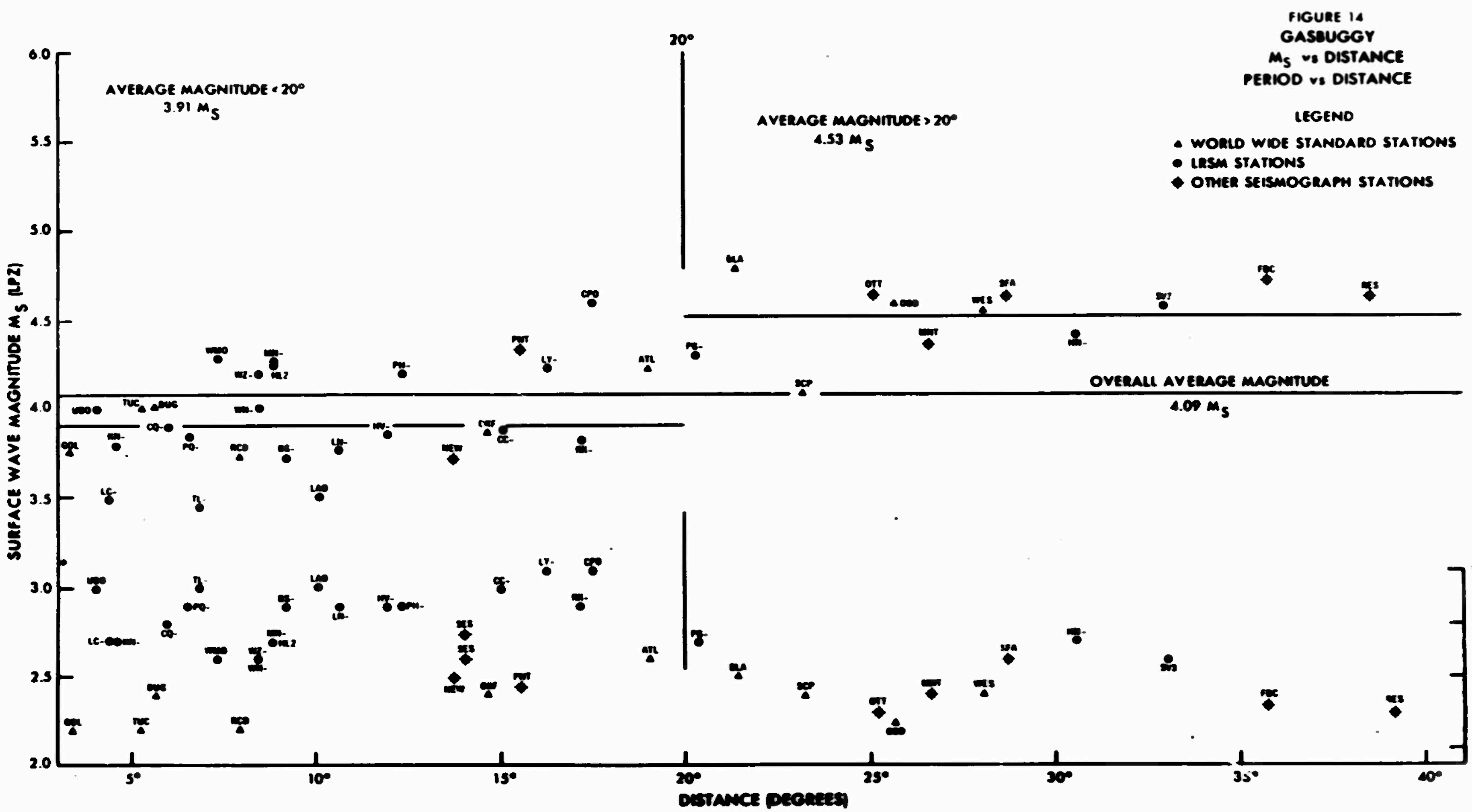
FIGURE 14
GASBUGGY
M_S vs DISTANCE
PERIOD vs DISTANCE
LEGEND
▲ WORLD WIDE STANDARD STATIONS
● LRSM STATIONS
◆ OTHER SEISMOGRAPH STATIONS
AVERAGE MAGNITUDE < 20°
3.91 M_S
AVERAGE MAGNITUDE > 20°
4.53 M_S
OVERALL AVERAGE MAGNITUDE
4.09 M_S
20°
SURFACE WAVE MAGNITUDE M_S (LPZ)
6.0
5.5
5.0
4.5
4.0
3.5
3.0
2.5
2.0
PERIOD (SEC.)
17
14
11
7
5°
10°
15°
20°
25°
30°
35°
40°
DISTANCE (DEGREES)

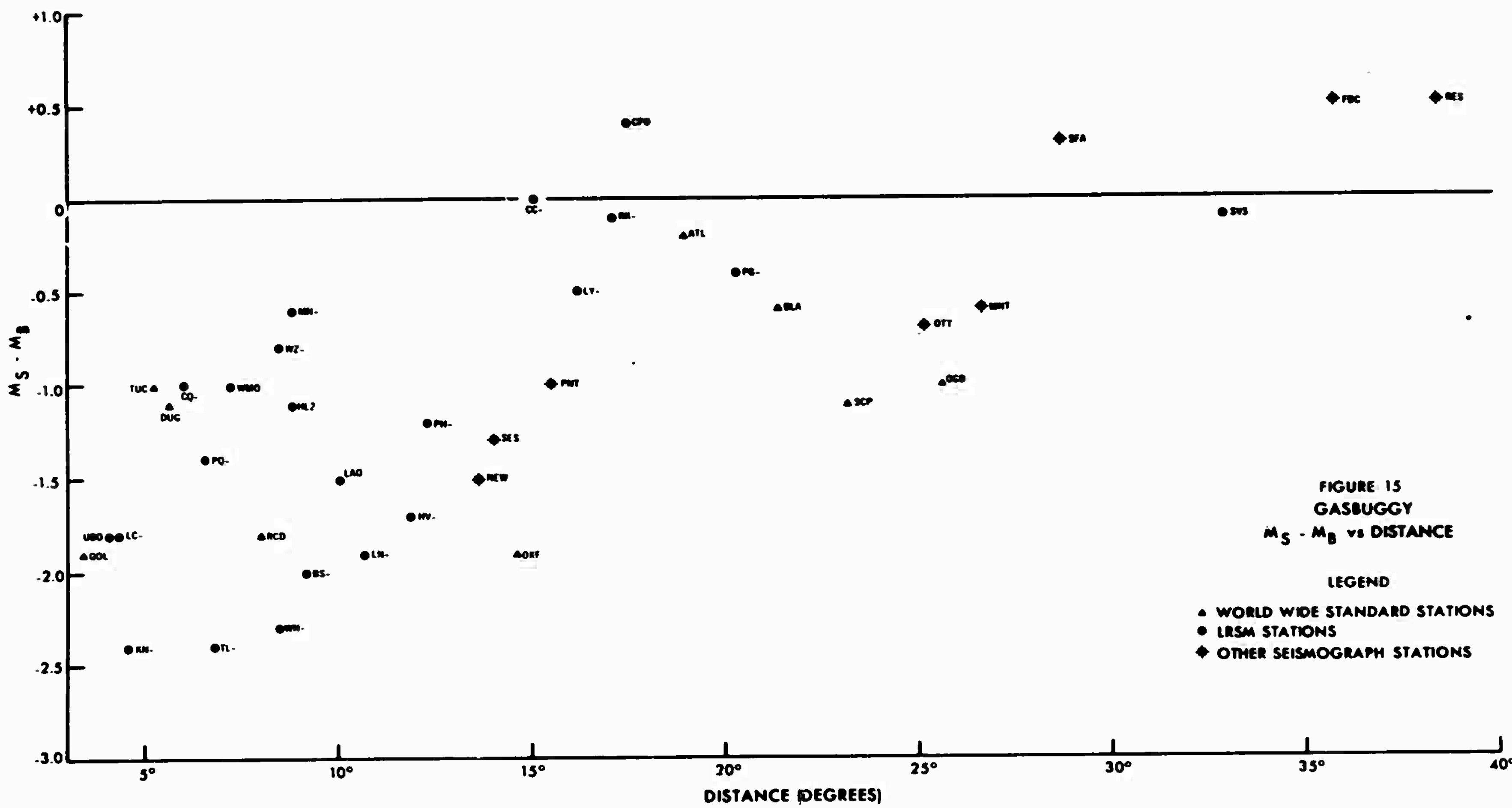

FIGURE 15
GASBUGGY
$M_S - M_B$ vs DISTANCE

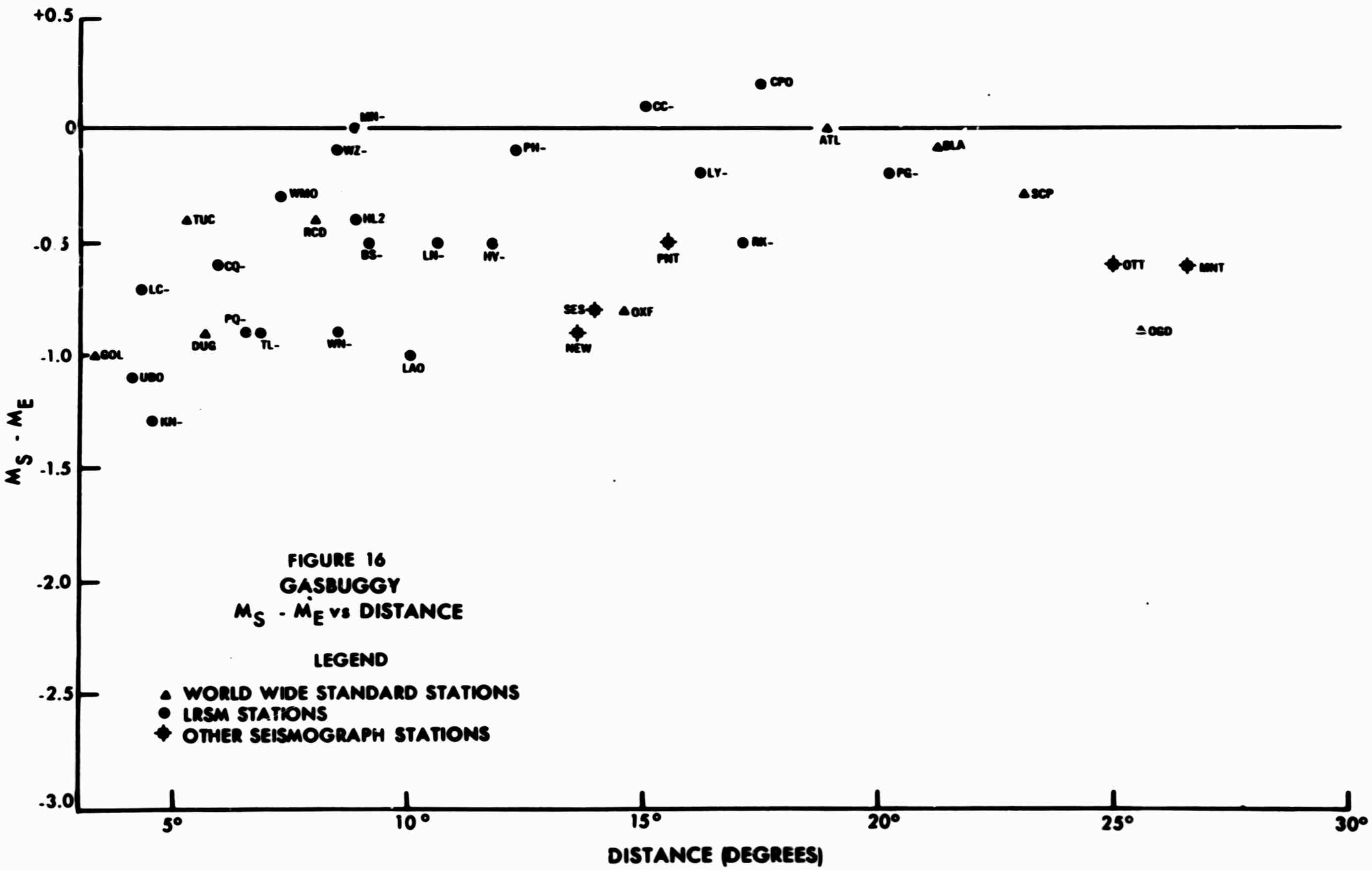

FIGURE 16
GASBUGGY
$M_S - \dot{M}_E$ vs DISTANCE

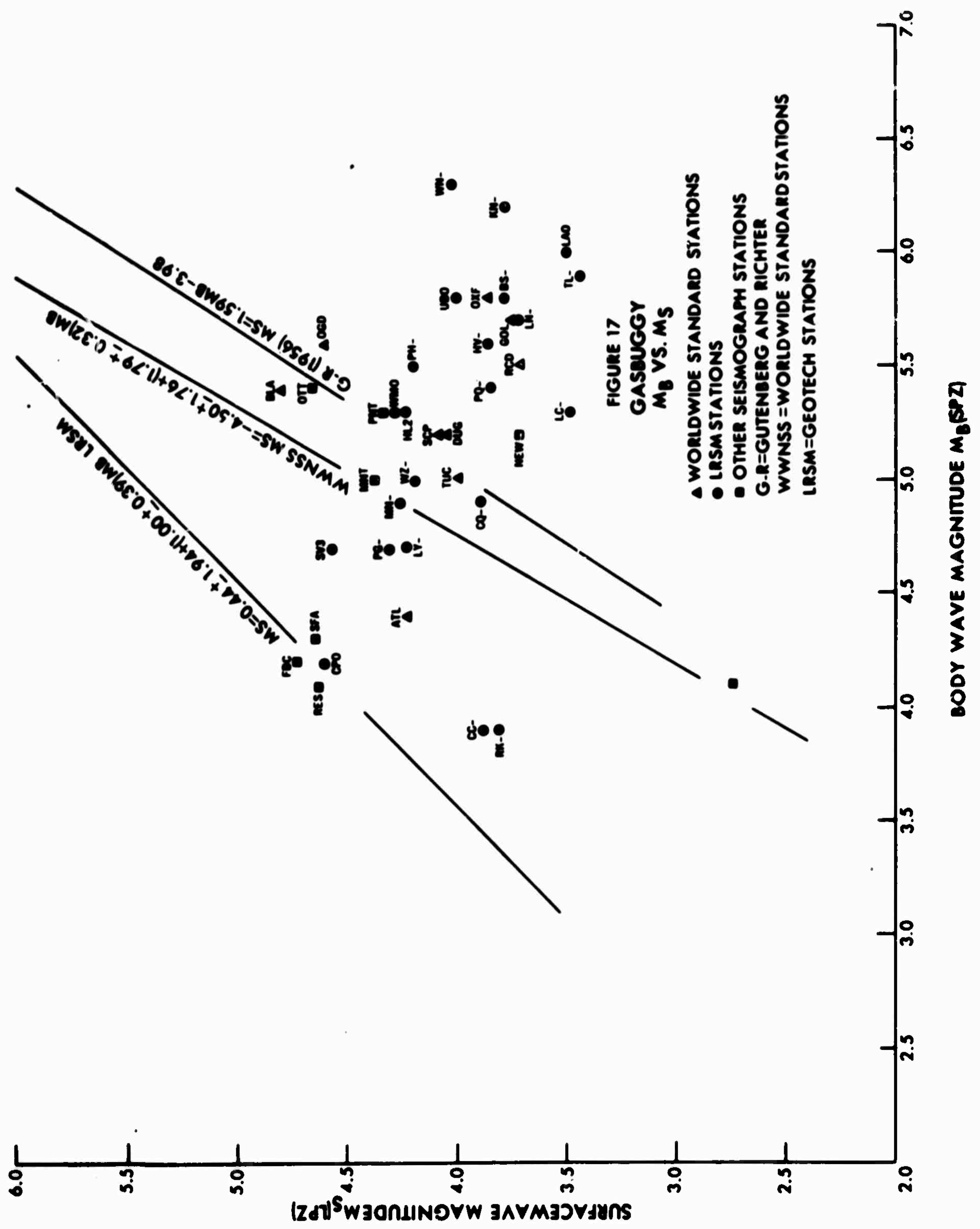

FIGURE 17
GASBUGGY
M_B VS. M_S

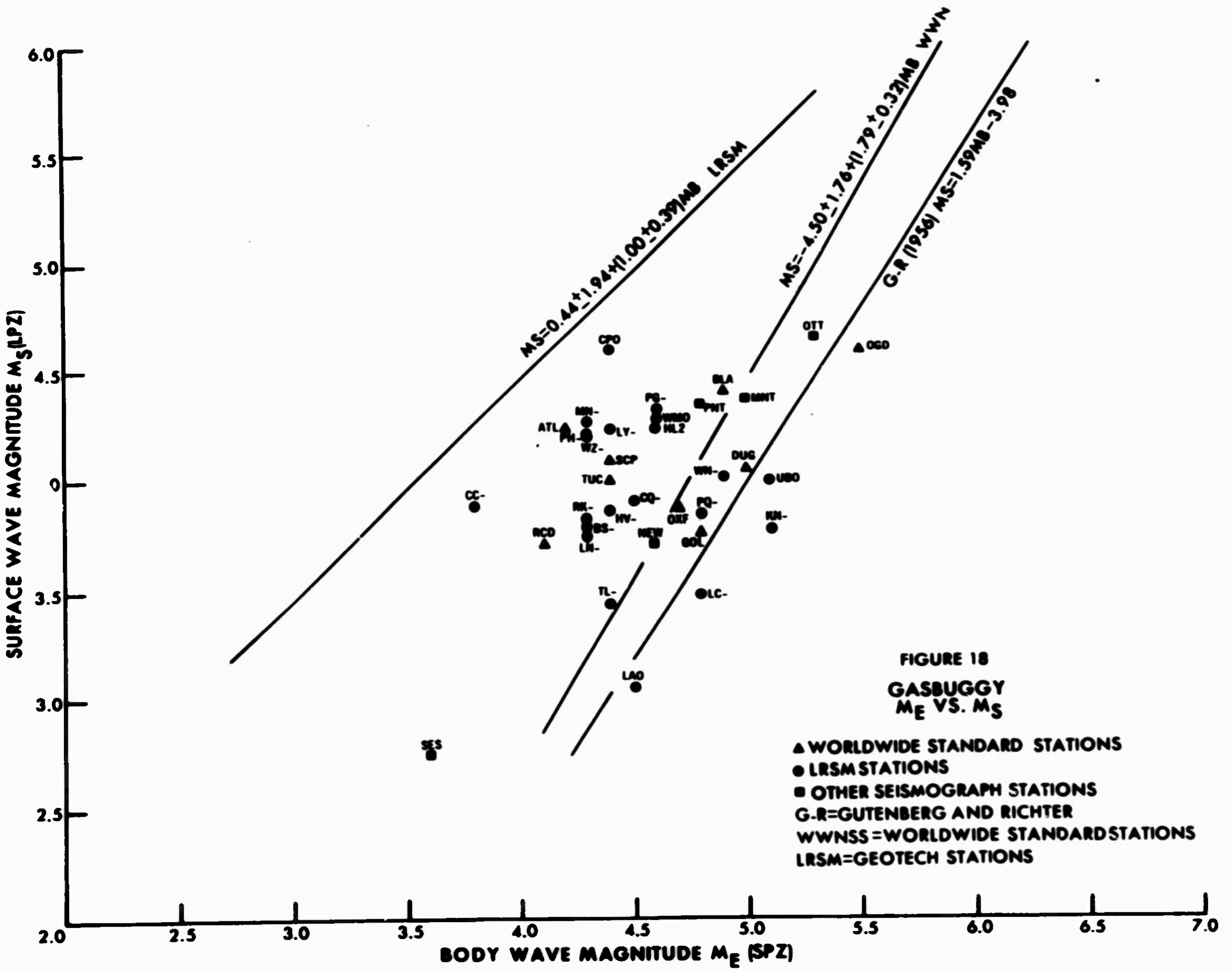

FIGURE 18

GASBUGGY
M_E VS. M_S

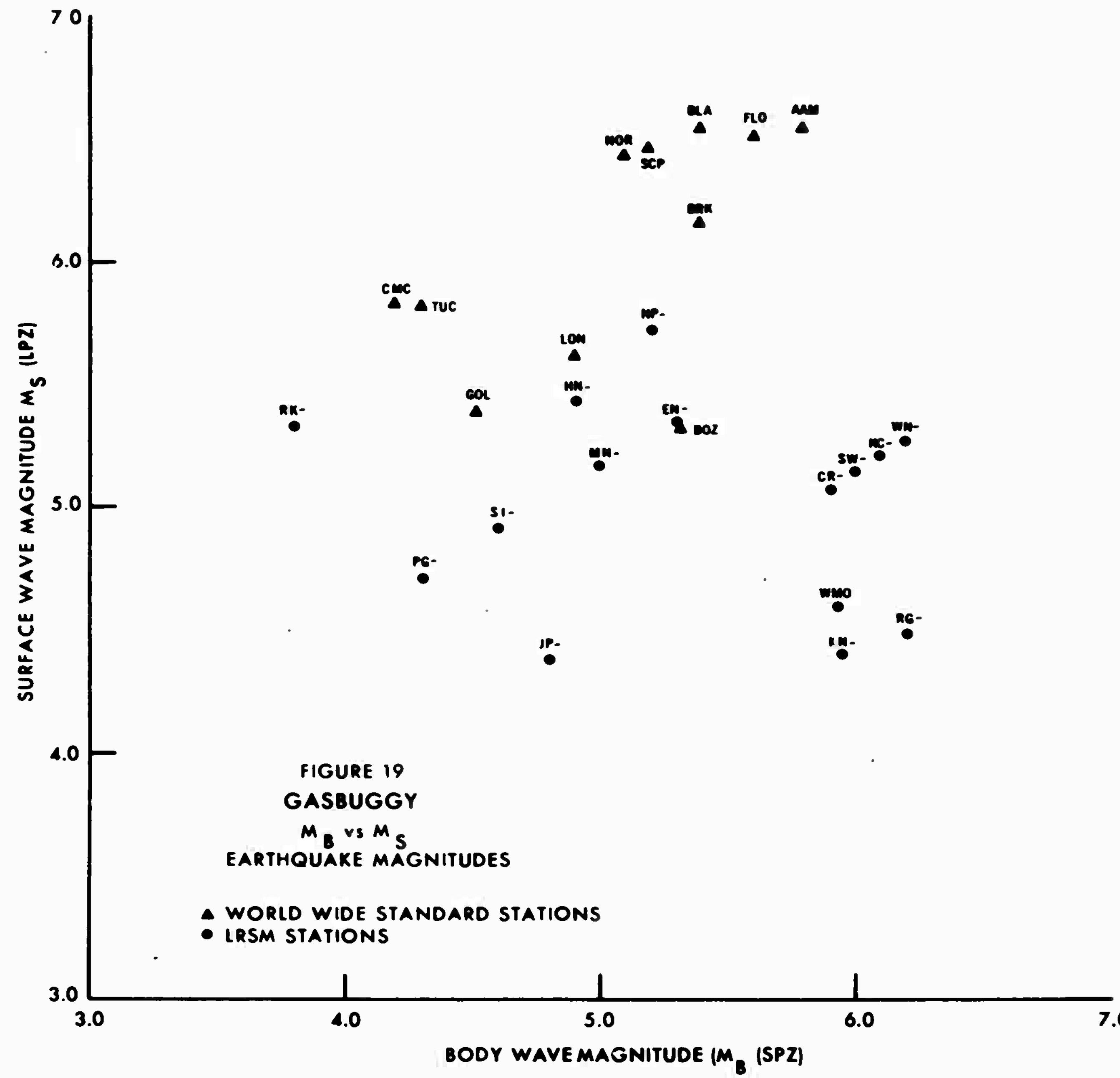

FIGURE 19
GASBUGGY
M_B vs M_S
EARTHQUAKE MAGNITUDES

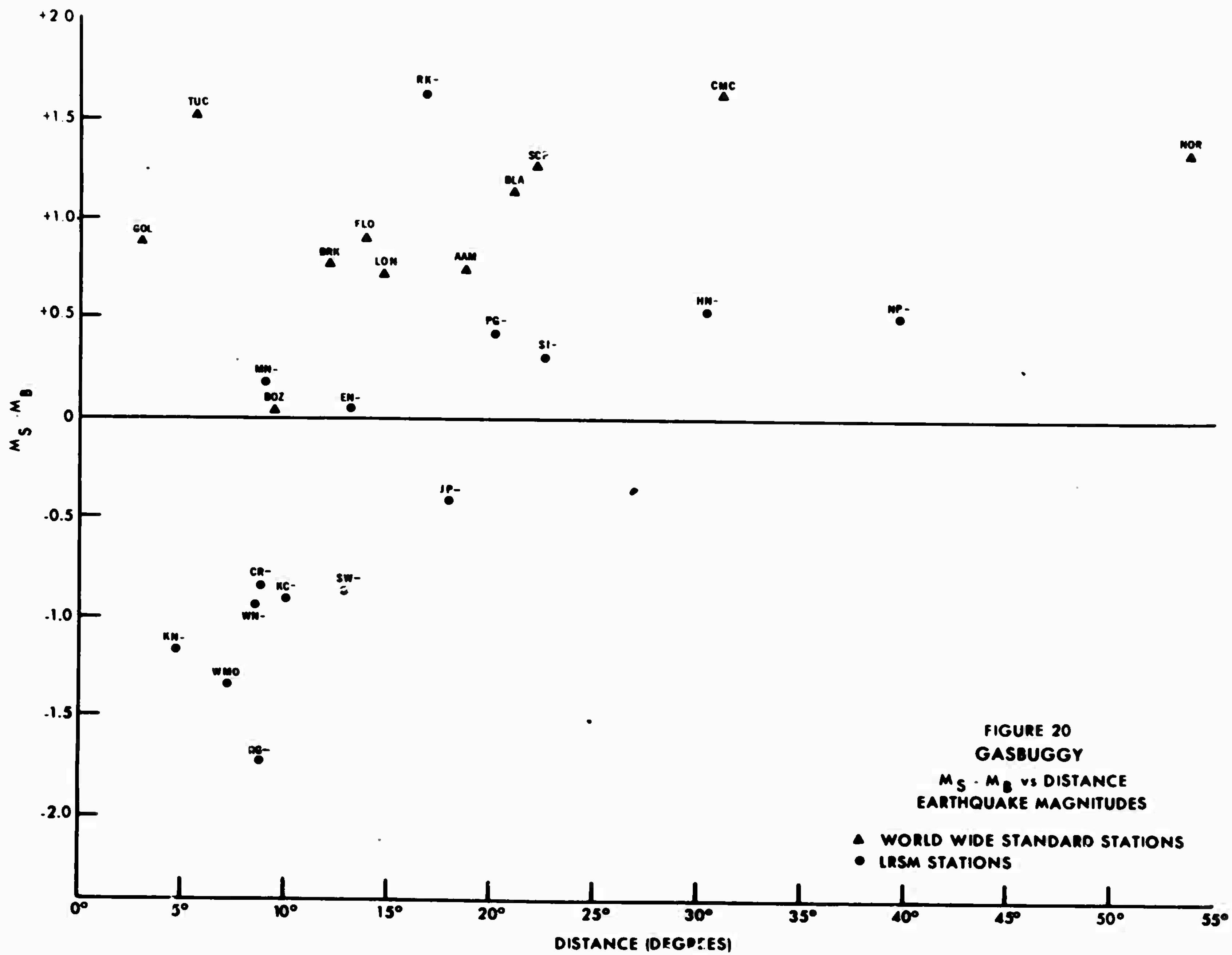

FIGURE 20
GASBUGGY
$M_S - M_B$ vs DISTANCE
EARTHQUAKE MAGNITUDES

Appendix I -- Temporary Seismograph Station Information Summary

Station	Latitude (N)	Longitude (W)	Distance Km.	Azimuth Deg.	Elevation feet	Instrumentation
IR1 Lindrith	36.304°	107.044°	44.0	160.4	7250	
IR2 Cuba	36.021°	106.958°	76.6	162.0	6900	
IR3 San Luis	35.680°	107.050°	111.6	172.0	6250	ASC-1
IR4 Puerco Dam	35.320°	107.039°	151.4	174.2	5780	ASC-1
IR5 Mesa Blanca	35.161°	107.039°	169.0	174.8	5920	ASC-1
IR6 South Garcia	34.877°	107.084°	200.2	176.7	5335	ASC-1
IR7 Mesa Aparejo	34.676°	107.106°	222.3	177.6	5900	ASC-1
IR8 Ladron Mountain	34.461°	107.033°	246.0	176.2	5700	ASC-2
R11 Bear Den School	33.368°	106.656°	370.7	172.0	5350	ASC-2
R12 Hembrillo	32.885°	106.681°	423.6	173.0	542[illegible]	ASC-2
R15 Taos	36.383°	105.551°	152.0	101.9	7200	ASC-2
R16 Mora Ranch	36.182°	104.904°	213.8	104.2	6950	ASC-2

Appendix 2 -- Q Tables for Specific Apparent Velocities

km	7.9 km/sec	ADJ	Q	8.1 km/sec	ADJ	Q	8.5 km/sec	ADJ		10.5 km/sec	ADJ	Q
0												
100												
200	70.0	700.0	2.155				450.0	4500.0	1.347			
300	150.0	1500.0	1.824				200.0	2000.0	1.699			
400	60.0	600.0	2.222	950.0	9500.0	1.022	400.0	400.0	2.398			
500	200.0	200.0	2.699	230.0	2300.0	1.638	700.0	700.0	2.156			
600	130.0	130.0	2.886	60.0	600.0	2.222	500.0	500.0	2.301			
700	75.0	75.0	3.125	20.0	200.0	2.699	370.0	370.0	2.432			
800	50.0	50.0	3.301	7.8	78.0	3.108	300.0	300.0	2.523			
900	36.0	36.0	3.444	3.2	32.0	3.495	230.0	230.0	2.638			
1000	27.0	27.0	3.568	1.7	17.0	3.770	180.0	180.0	2.744			
1100	20.0	20.0	3.699	.85	8.5	4.071	160.0	160.0	2.796			
1200	16.0	16.0	3.796	.45	4.5	4.346	140.0	140.0	2.854			
1300				.26	2.6	4.585	120.0	120.0	2.921			
1400				.16	1.6	4.796	99.0	99.0	3.001			
1500				(.1)	(1.0)	(5.000)	84.0	84.0	3.076			
1600							72.0	72.0	3.143	370.0	370.0	2.431
1700							65.0	65.0	3.188	290.0	290.0	2.538
1800							58.0	58.0	3.238	240.0	240.0	2.620
1900							51.0	51.0	3.293	180.0	180.0	2.744
2000							48.0	48.0	3.318	160.0	160.0	2.796
2100										140.0	140.0	2.854
2200										100.0	100.0	3.000
2300										85.0	85.0	3.071
2400										70.0	70.0	3.155
2500										60.0	60.0	3.222
2600										50.0	50.0	3.301
2700										44.0	44.0	3.357
2800										38.0	38.0	3.421
2900										33.0	33.0	3.482
3000										28.0	28.0	3.553

$M_{B_{P_{SPZ}}} = Q + q + S$

where

$M = 5$

Q = Distance factor

$q = \log_{10} A/T$ ($m\mu$/sec)

$S = 0$

$5 = Q + q$ (from Page 632)